



University
of Glasgow

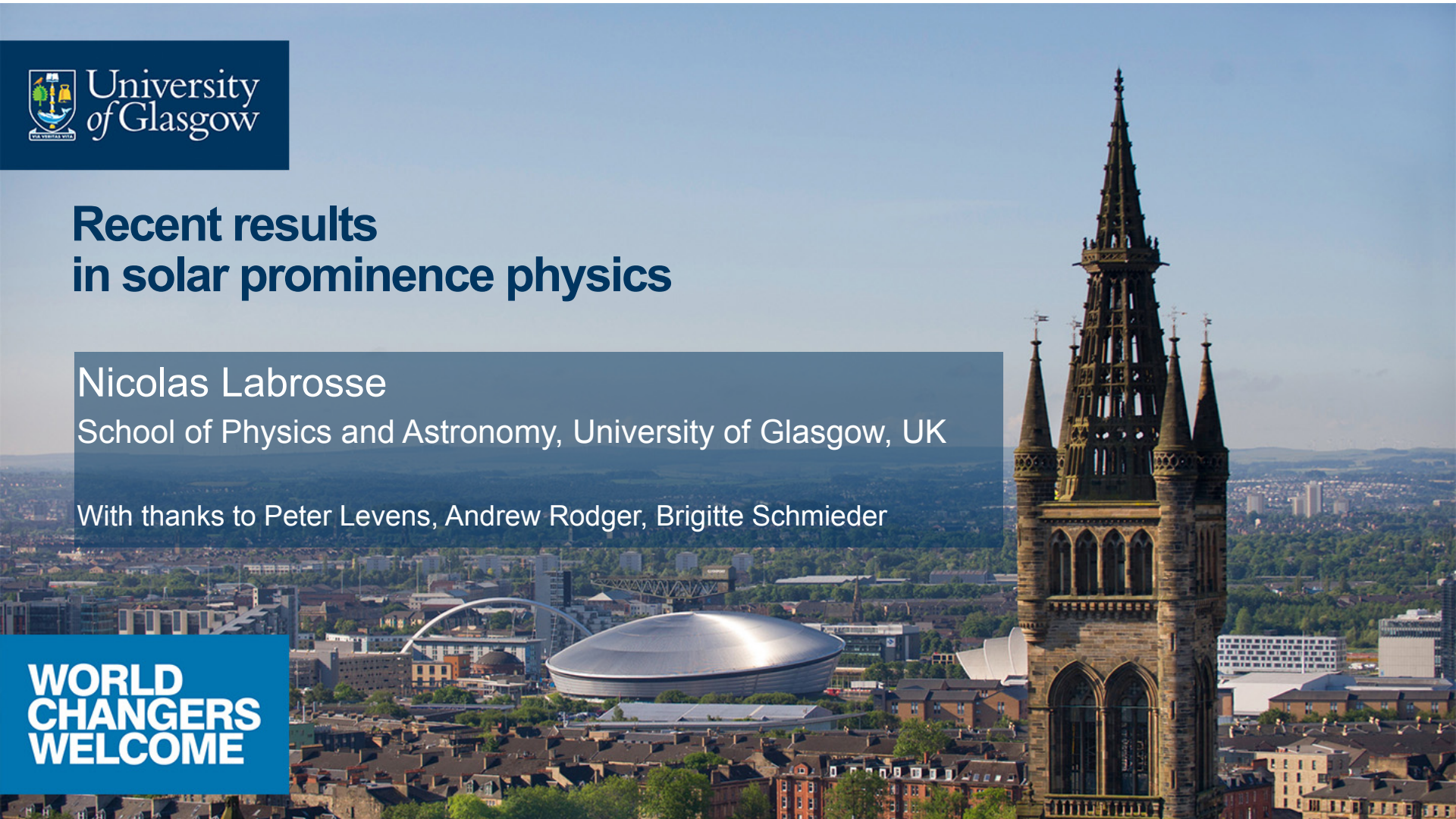
Recent results in solar prominence physics

Nicolas Labrosse

School of Physics and Astronomy, University of Glasgow, UK

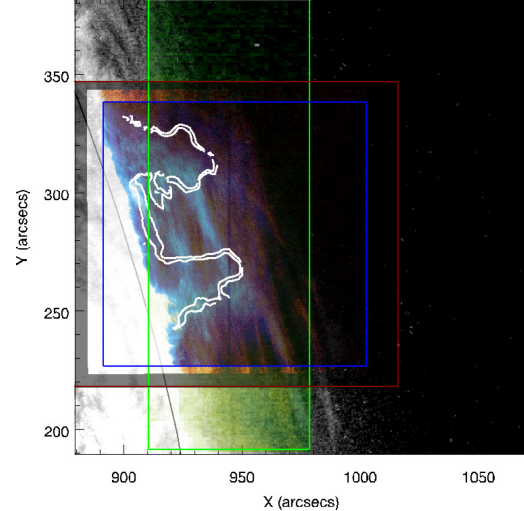
With thanks to Peter Levens, Andrew Rodger, Brigitte Schmieder

**WORLD
CHANGERS
WELCOME**

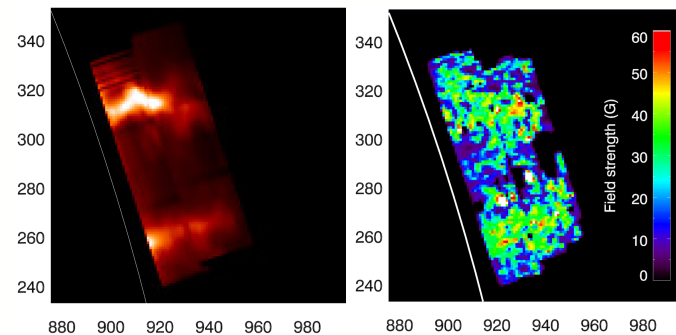


July 2014
Observations

SOT Ca II H



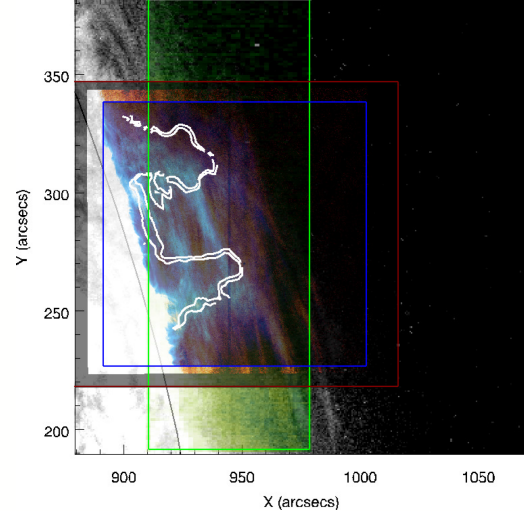
Levens et al (2016, 2017)



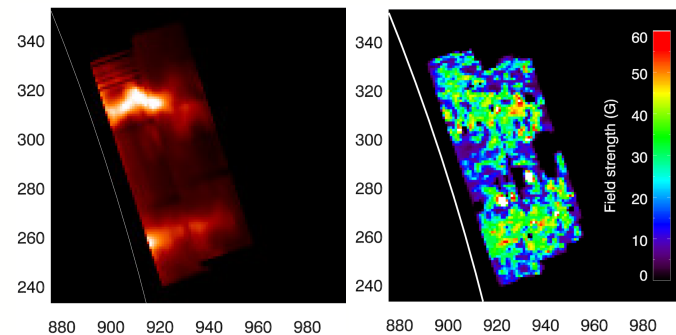
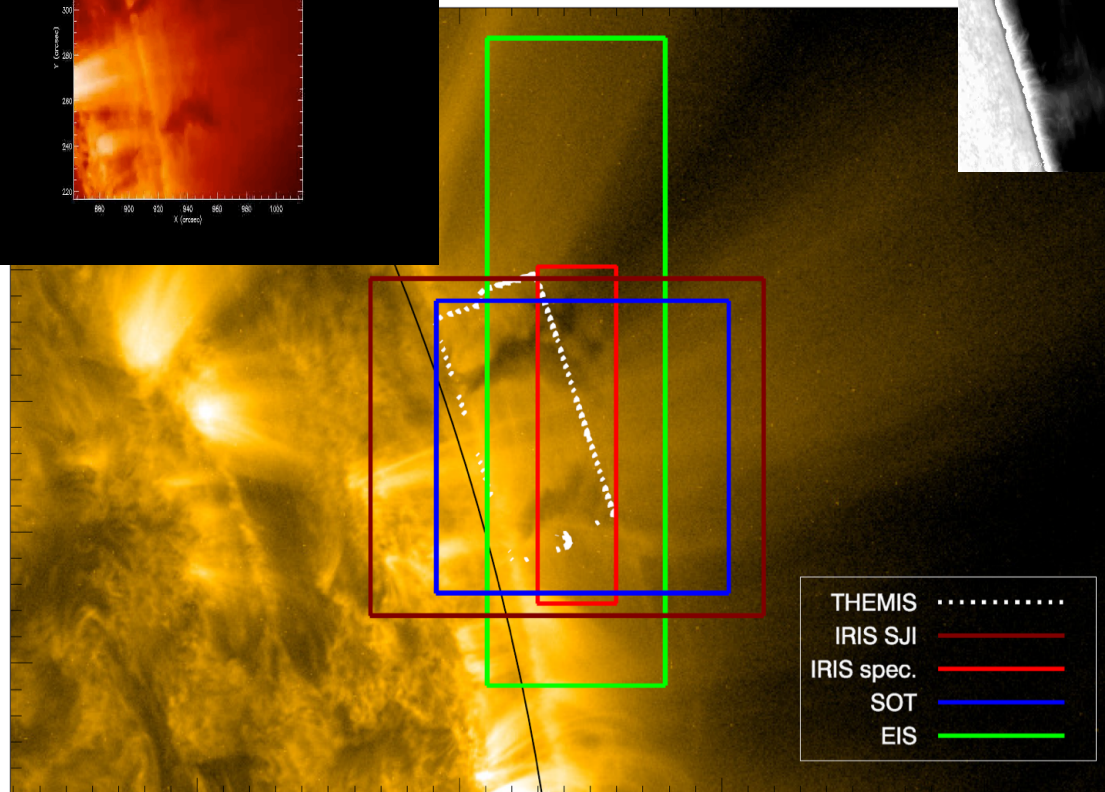
THEMIS He I D3 and B strength

July 2014
Observations

SOT Ca II H



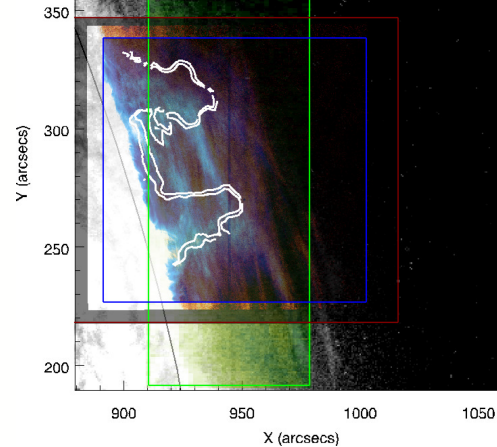
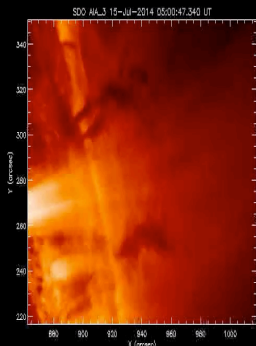
Levens et al (2016, 2017)



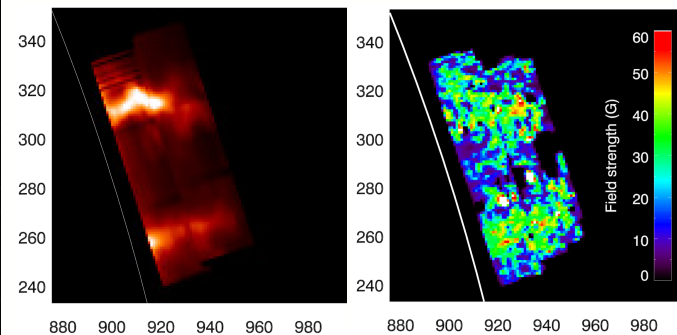
THEMIS He I D3 and B strength

AIA 171

SOT Ca II H



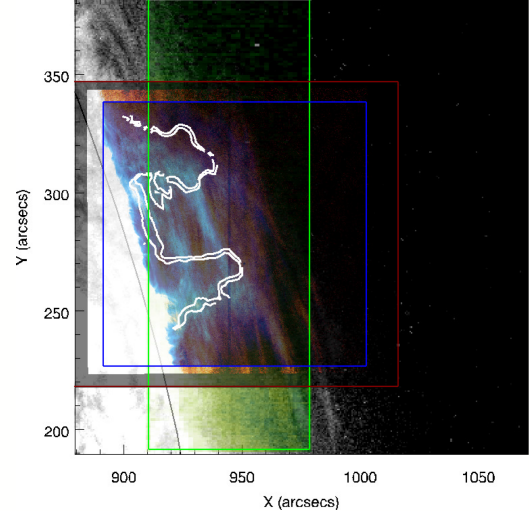
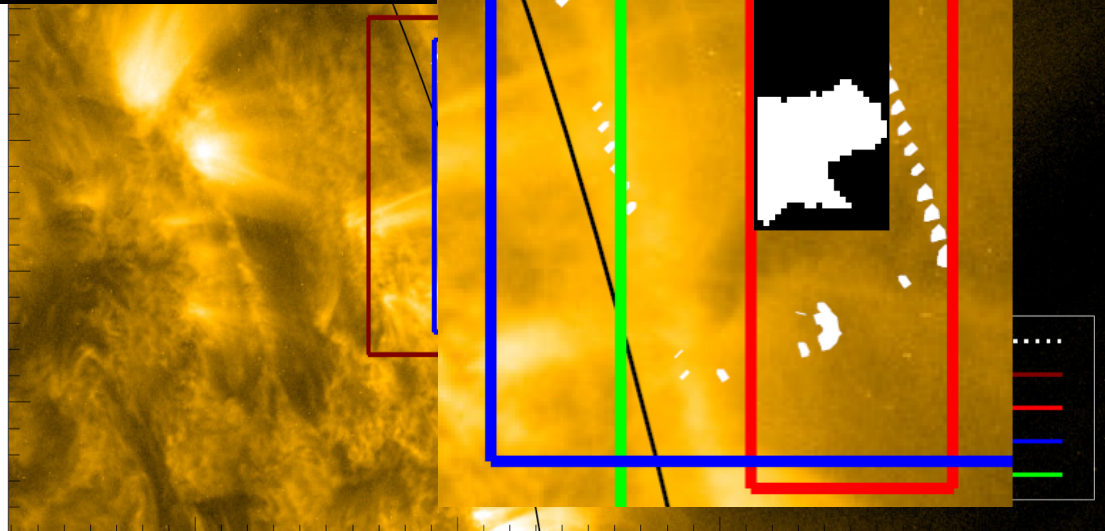
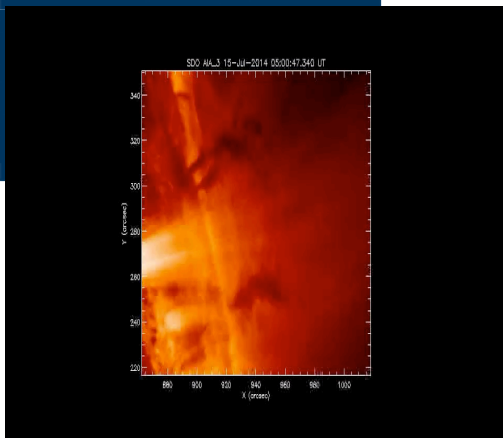
Levens et al (2016, 2017)



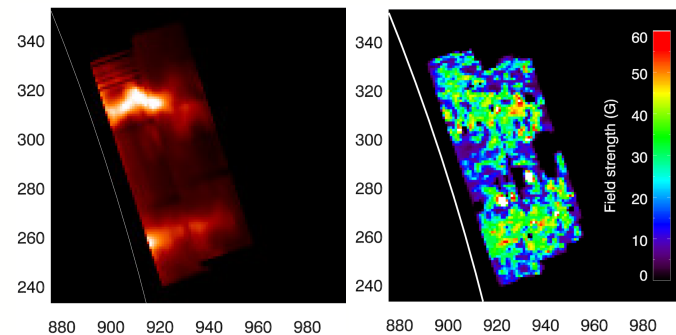
THEMIS He I D3 and B strength

AIA 171

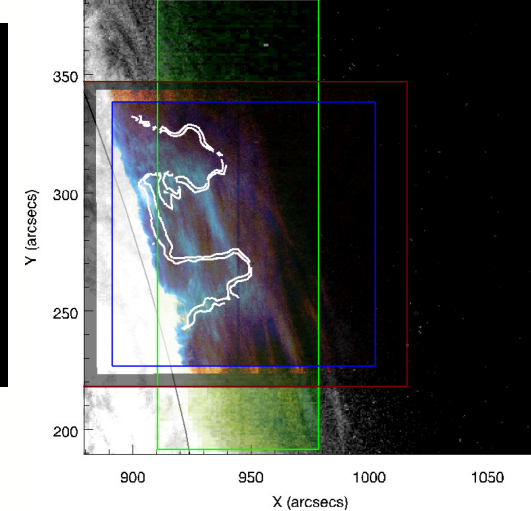
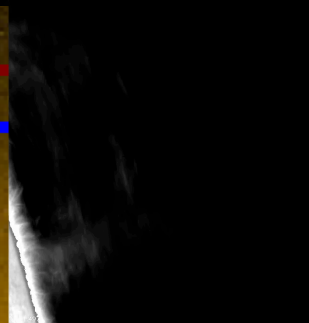
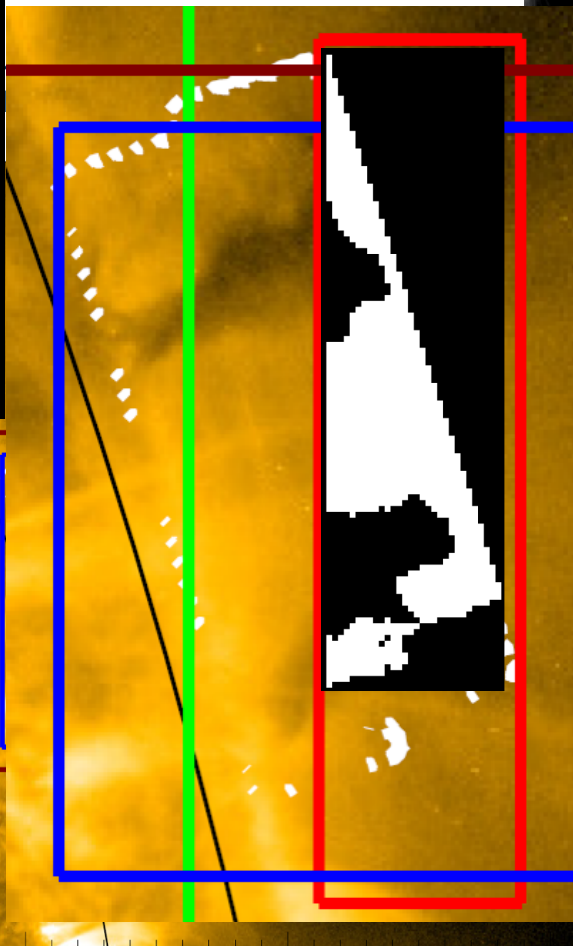
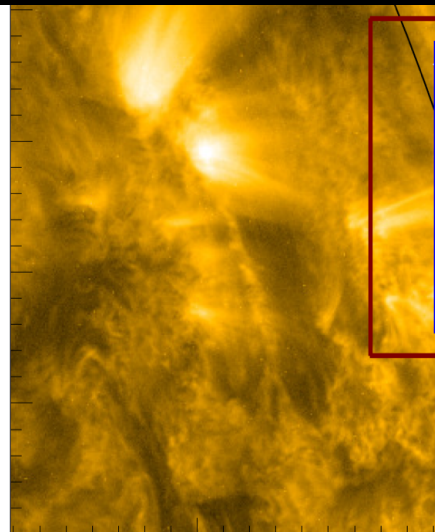
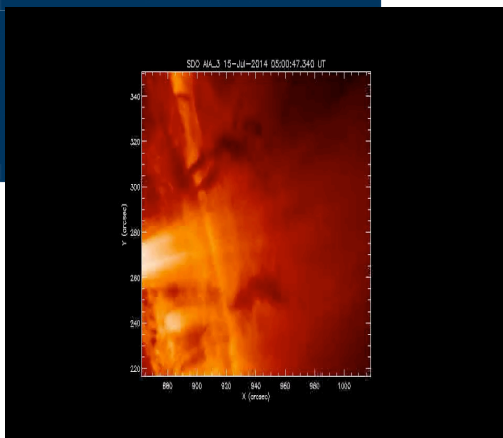
SOT Ca II H



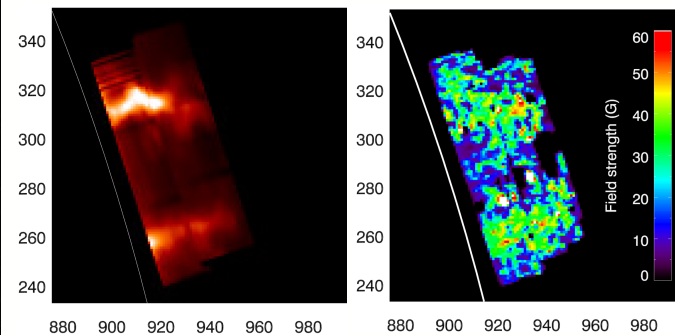
Levens et al (2016, 2017)



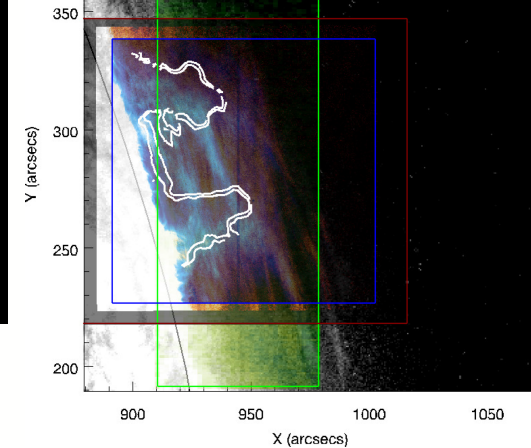
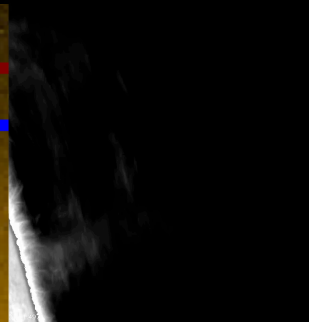
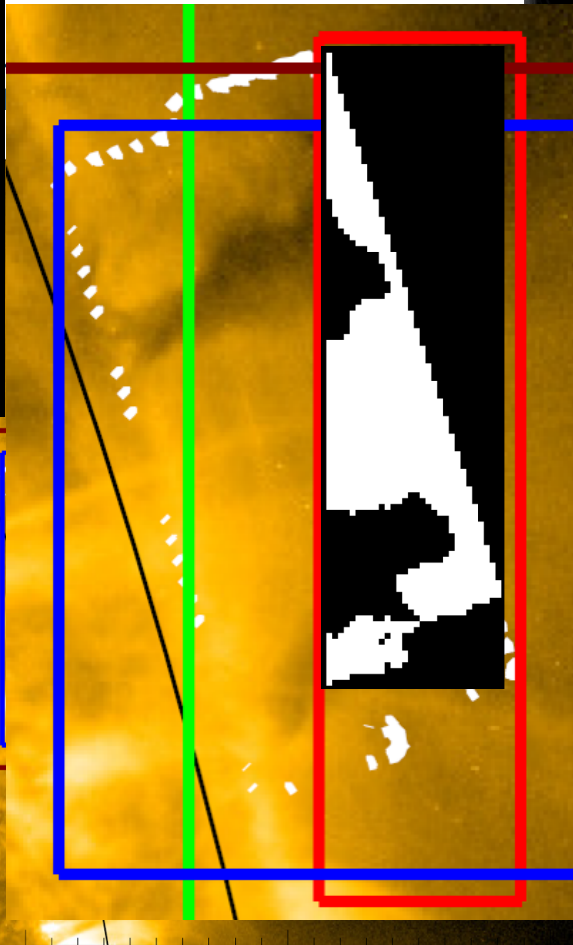
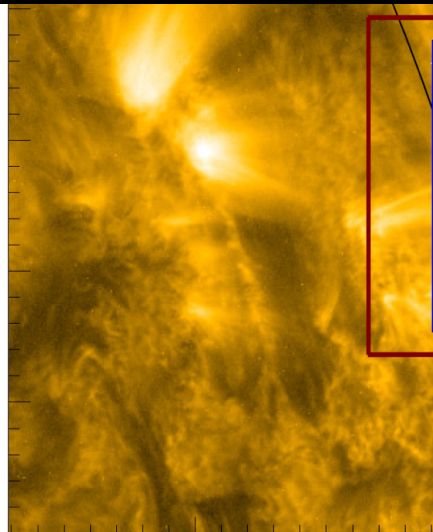
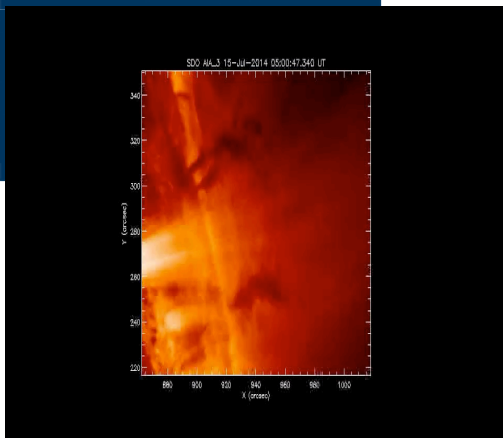
THEMIS He I D3 and B strength



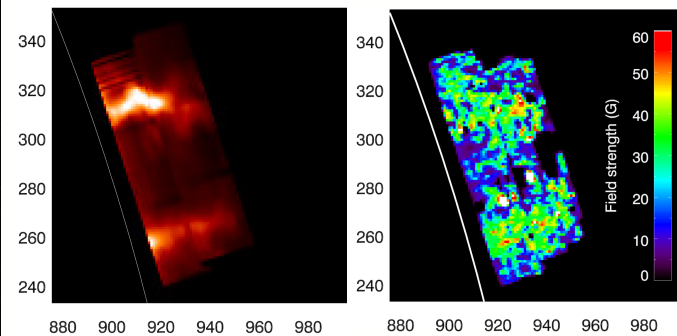
Levens et al (2016, 2017)



THEMIS He I D3 and B strength



Levens et al (2016, 2017)



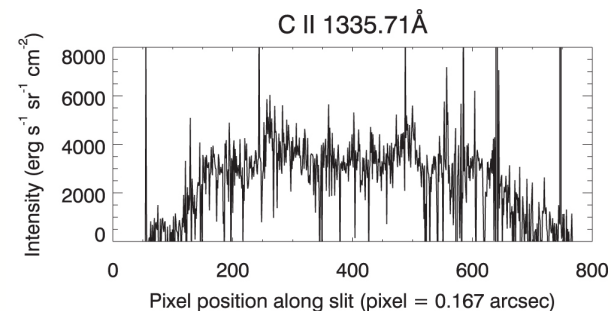
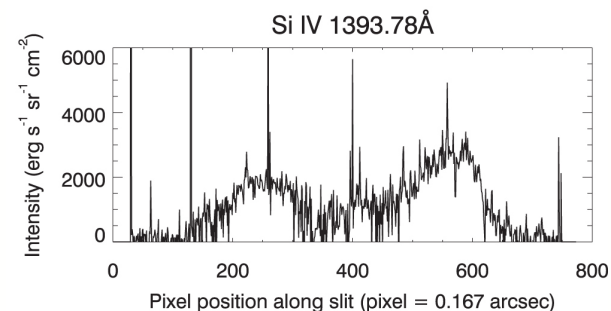
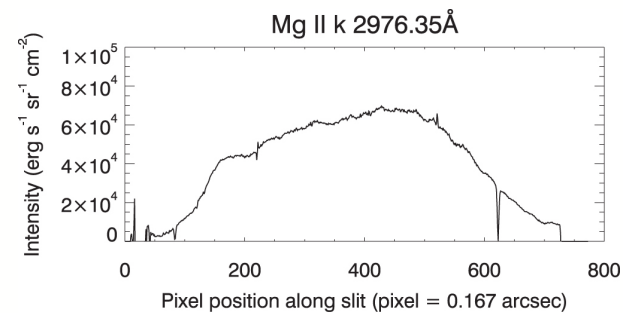
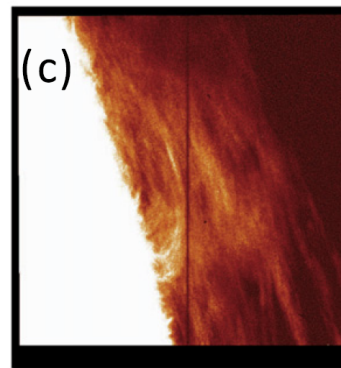
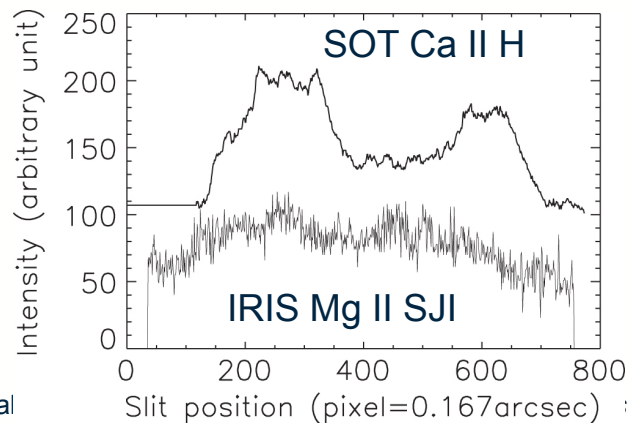
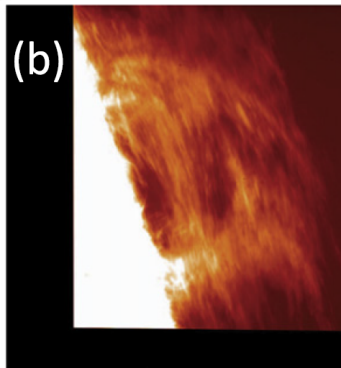
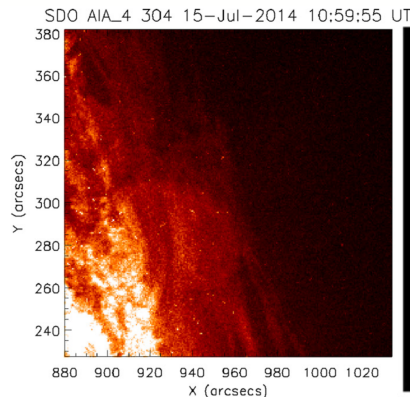
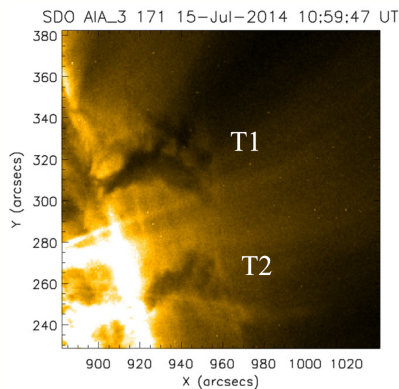
THEMIS He I D3 and B strength



University
of Glasgow

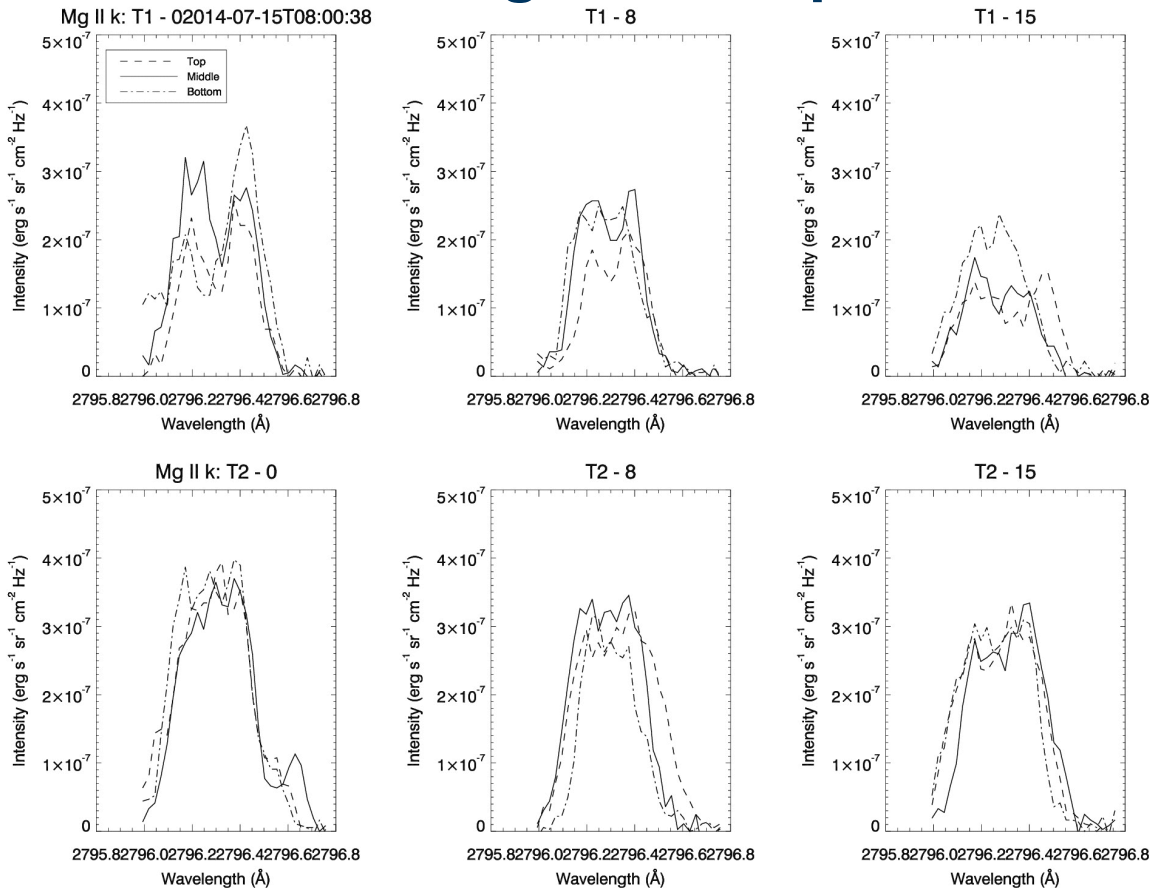
Joint observations

Levens et al (2016)



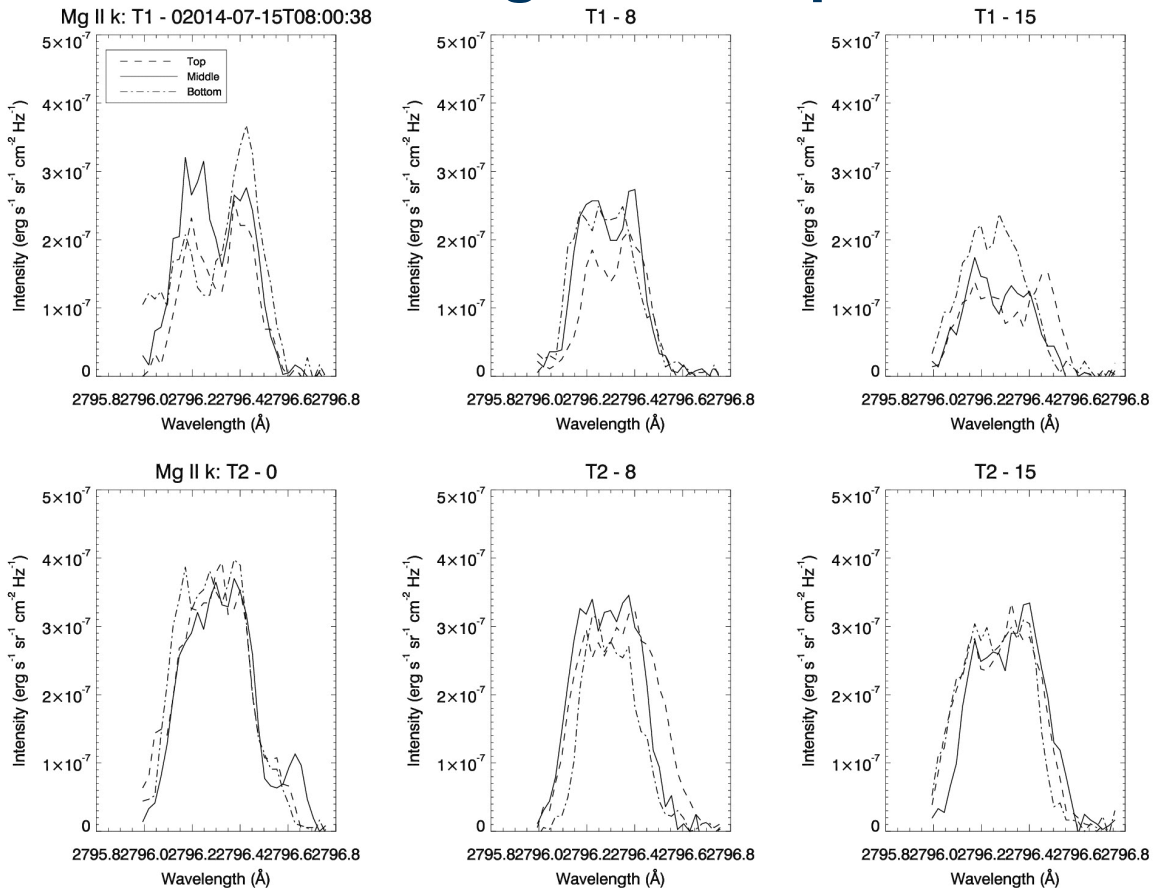


Observations of Mg II lines in prominences with IRIS





Observations of Mg II lines in prominences with IRIS





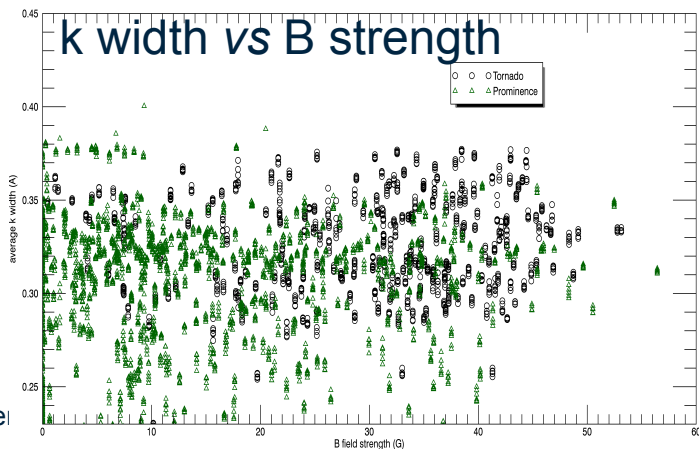
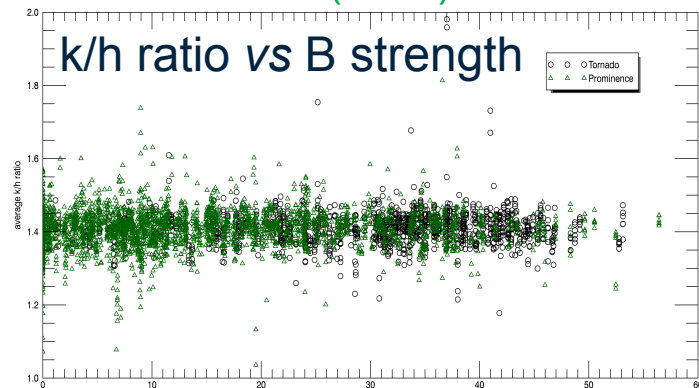
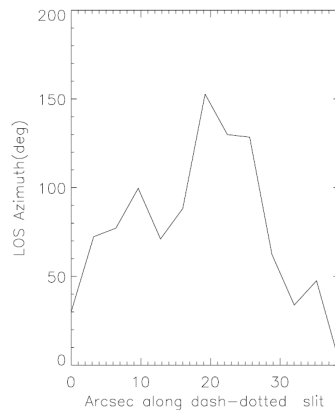
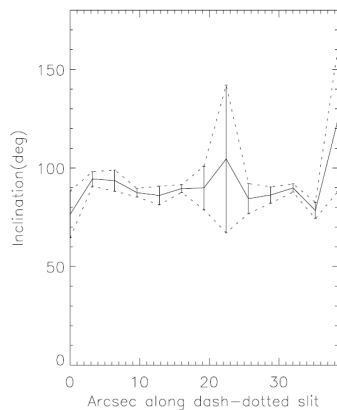
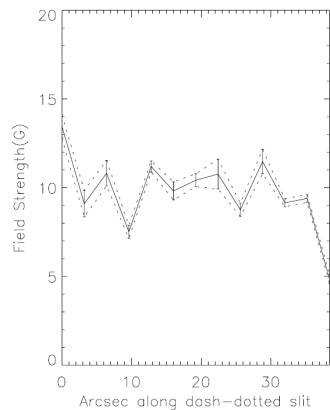
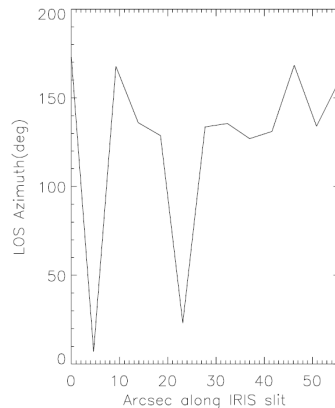
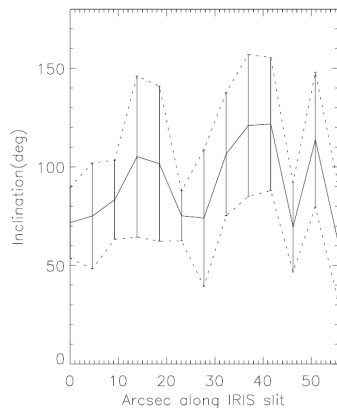
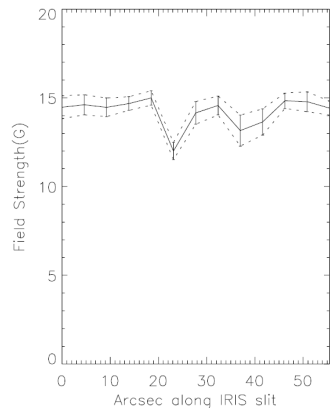
University
of Glasgow

Plasma and magnetic field

No correlation between Mg II line parameters and B strength

Schmieder et al (2014)

Levens et al (2017)



No tornado rotation

Levens et al (2016)

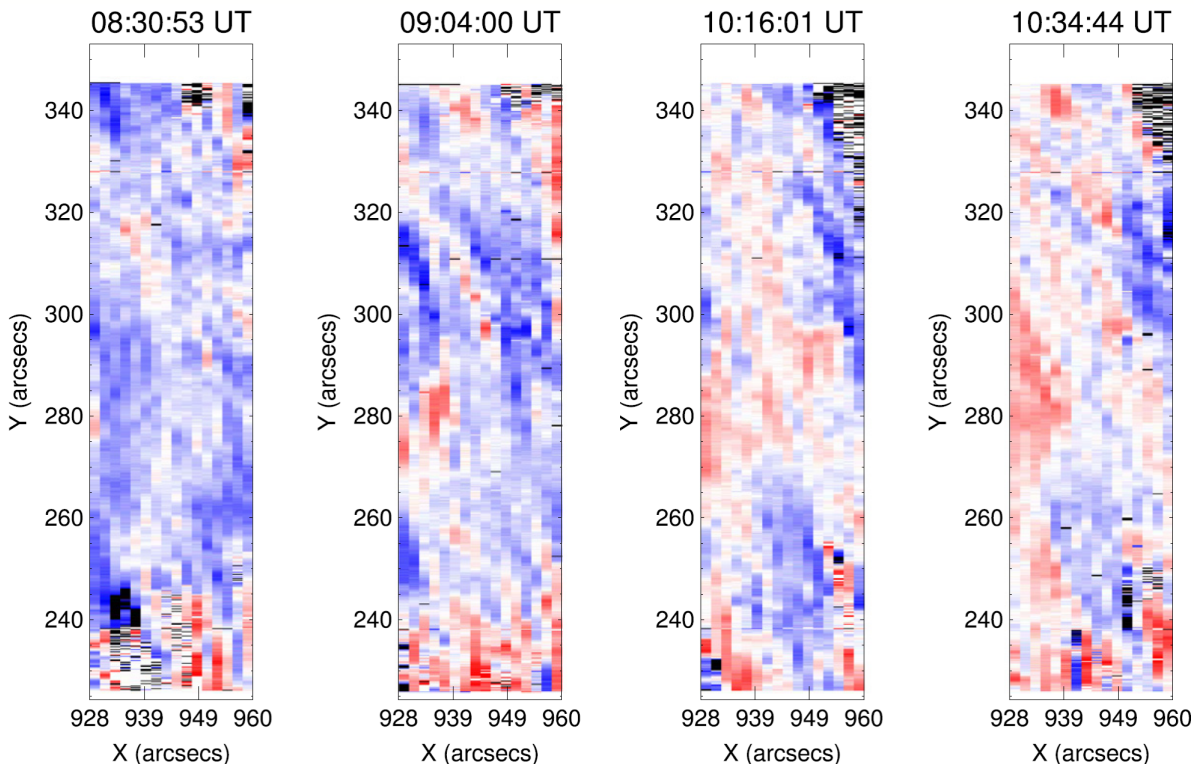
No evidence for rotation in Mg II k line.

Time–distance analysis of AIA images reveals that there are oscillations in the two tornadoes over a period of around 1–1.5 hr.

What mechanism causes these oscillations remains unknown.

See also Kucera et al (2018)

IRIS Mg II k doppler velocities



No tornado rotation

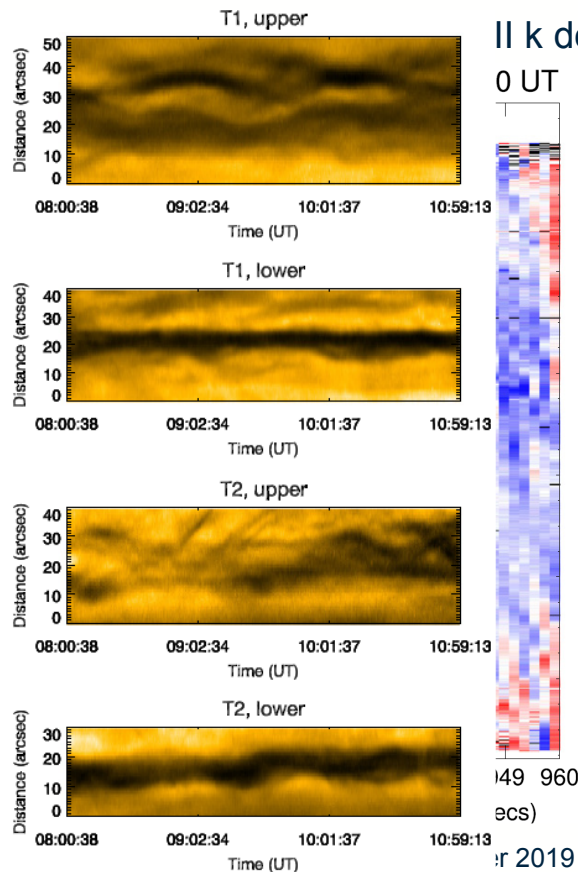
No evidence for rotation in Mg II k line.

Time–distance analysis of AIA images reveals that there are oscillations in the two tornadoes over a period of around 1–1.5 hr.

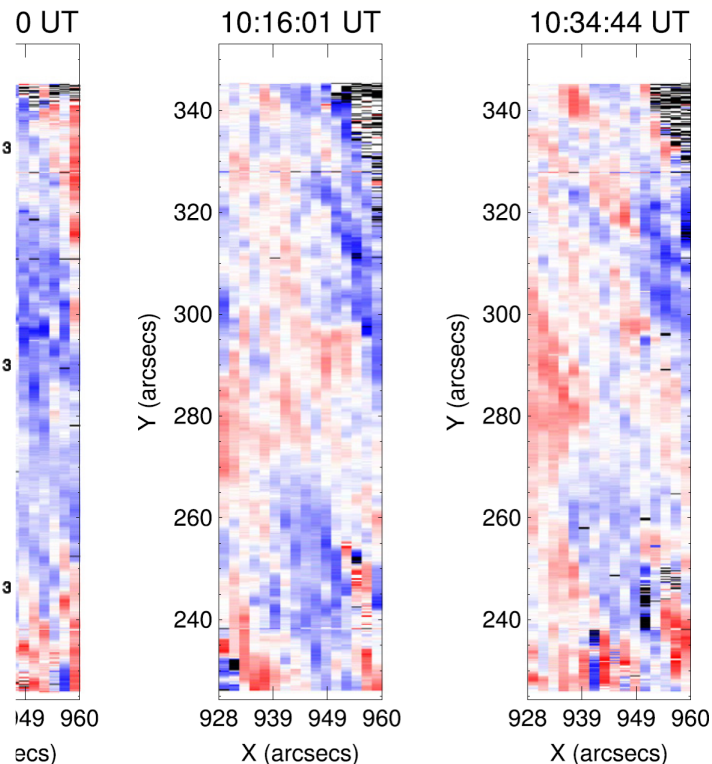
What mechanism causes these oscillations remains unknown.

See also [Kucera et al \(2018\)](#)

[Levens et al \(2016\)](#)



II k doppler velocities



Limits $\sim \pm 10$ km/s

Models

1D plane-parallel non-LTE radiative transfer code to compute Mg II lines (Levens & Labrosse 2019)

- prominence to corona transition region (PCTR)
- detailed incident radiation from IRIS

Similar to recent 1D prominence Mg II models by Heinzel et al (2014,2015) but with finer grid of parameters

- ⇒ Study line formation mechanisms
- ⇒ Explore model grid to compare with observations

Models

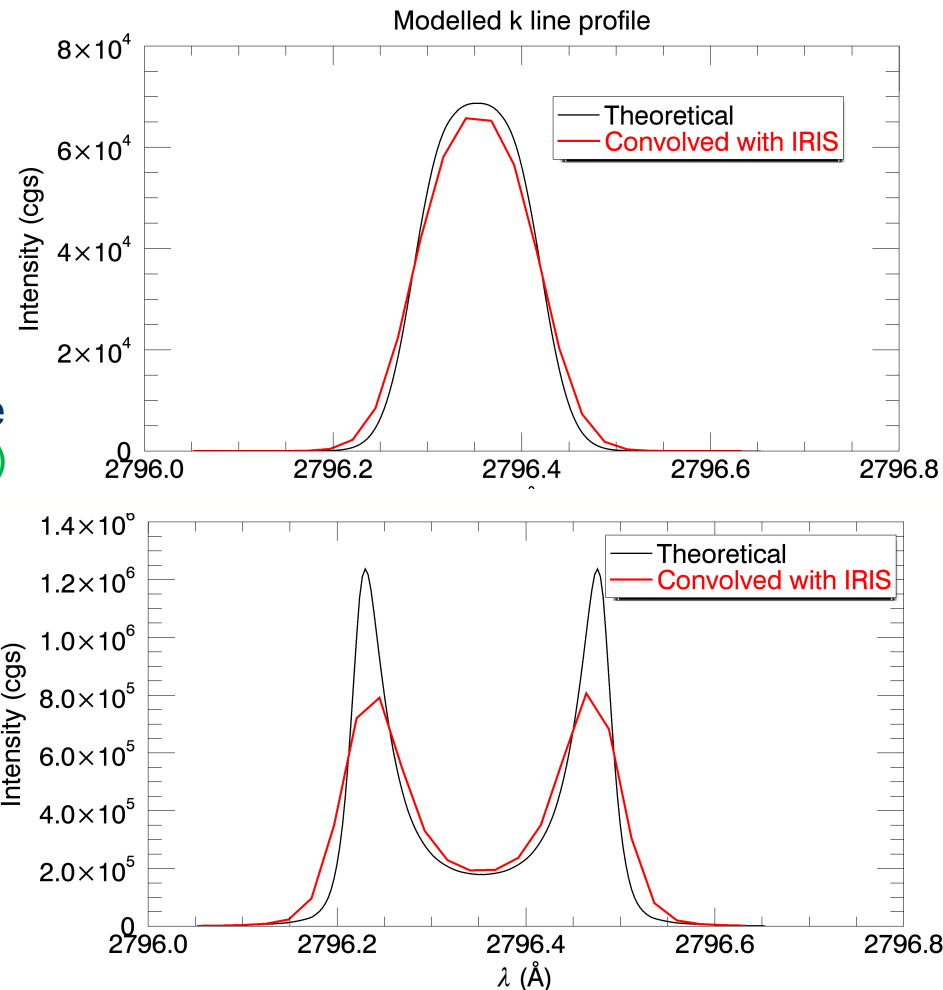
Two examples of k line profile showing result of convolution with instrumental profile + rebinning to IRIS spectral pixel size

1D plane-parallel non-LTE radiative transfer code to compute Mg II lines (Levens & Labrosse 2019)

- prominence to corona transition region (PCTR)
- detailed incident radiation from IRIS

Similar to recent 1D prominence Mg II models by Heinzel et al (2014,2015) but with finer grid of parameters

⇒ Study line formation mechanisms
⇒ Explore model grid to compare with observations





University
of Glasgow

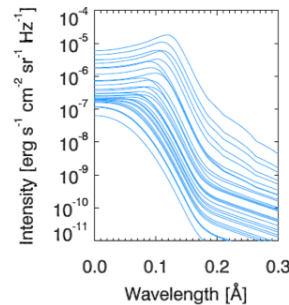
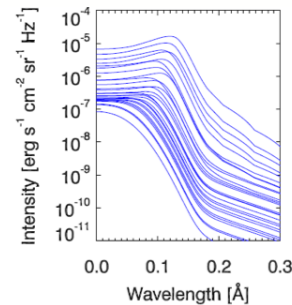
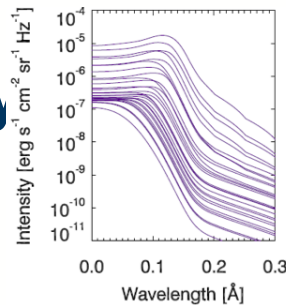
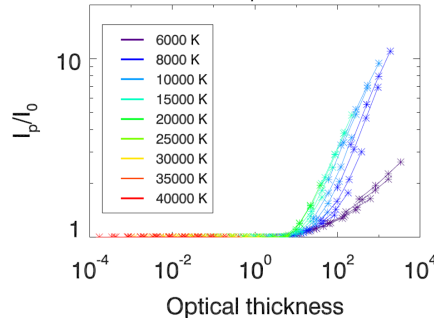
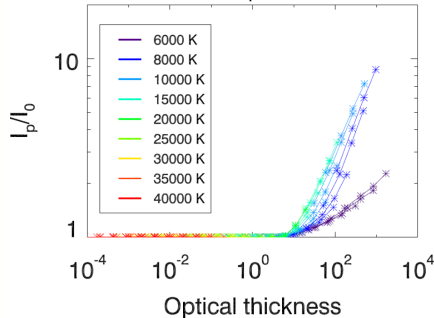
What do models say

Levens & Labrosse (2019)

Mg II h - I_p/I_0 vs. τ

No PCTR

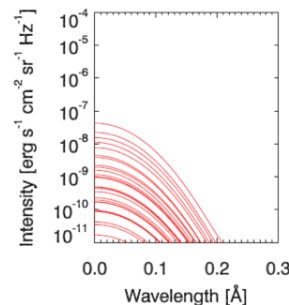
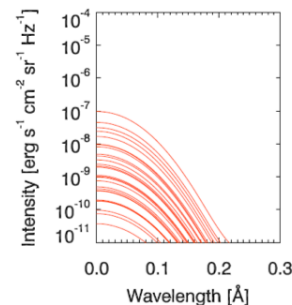
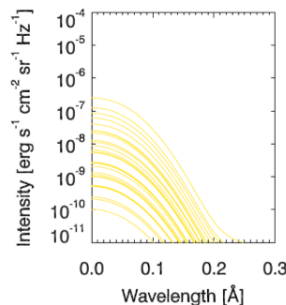
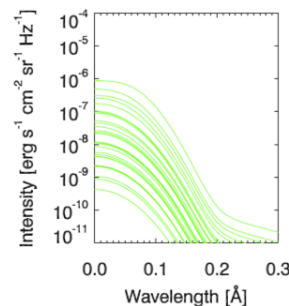
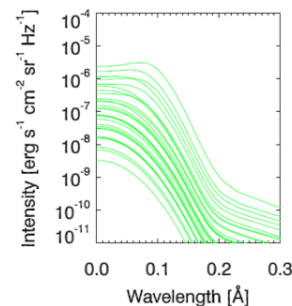
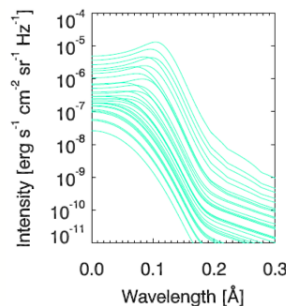
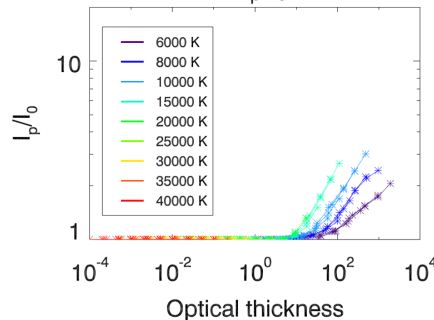
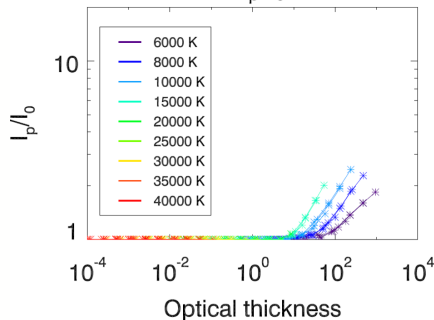
Mg II k - I_p/I_0 vs. τ



Mg II h - I_p/I_0 vs. τ

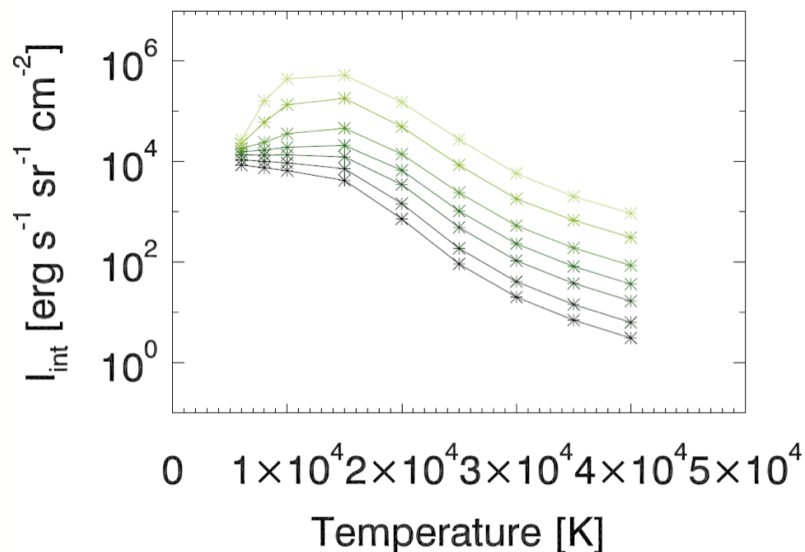
With PCTR

Mg II k - I_p/I_0 vs. τ

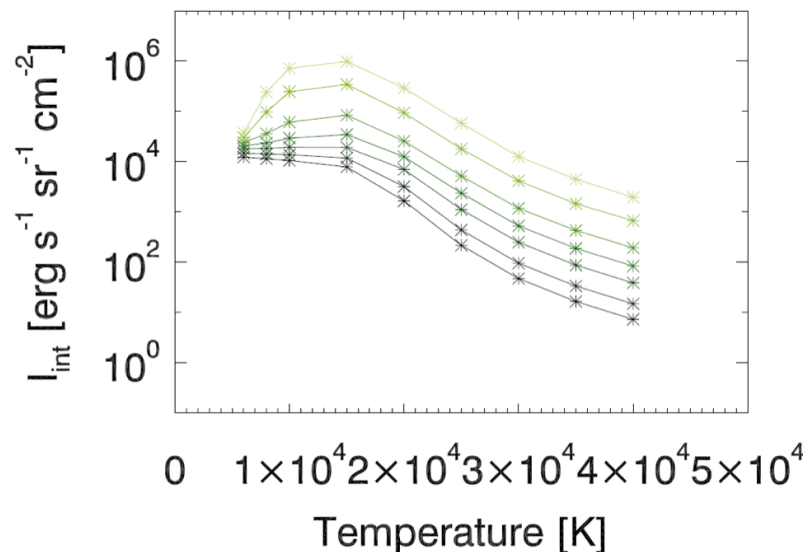


Integrated intensities

Mg II h - I_{int} vs. Temperature



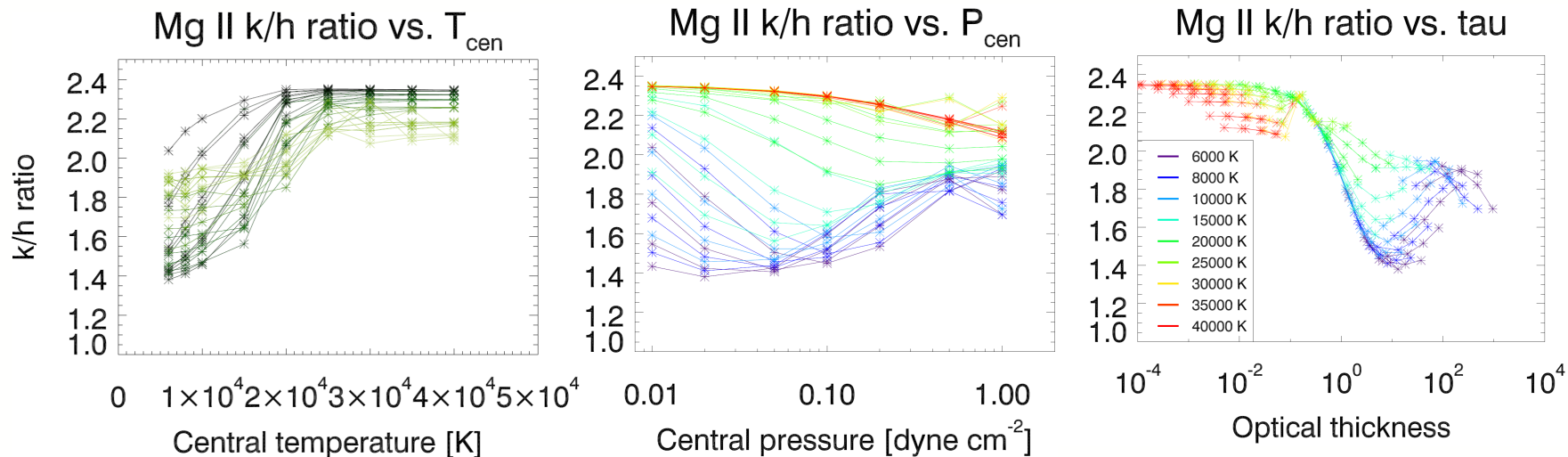
Mg II k - I_{int} vs. Temperature



Importance of radiative excitation means that photons of Mg II h and k are created at around 10 000 K, ie much lower temperature than estimated from pure collisional excitation.

Plasma diagnostics

Our 1D NLTE modelling of Mg II suggests that most prominences emitting in Mg II h and k lines are cold, low pressure, and optically thick structures (Levens & Labrosse 2019).





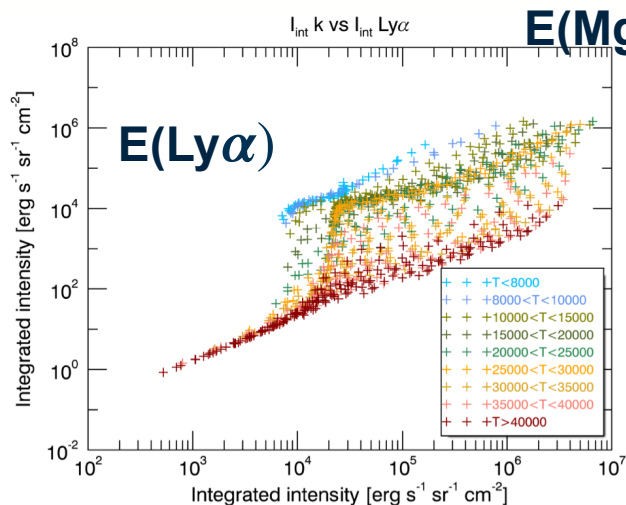
University
of Glasgow

Correlations between Mg II k and hydrogen line intensities, as well as with the emission measure (Levens & Labrosse 2019).

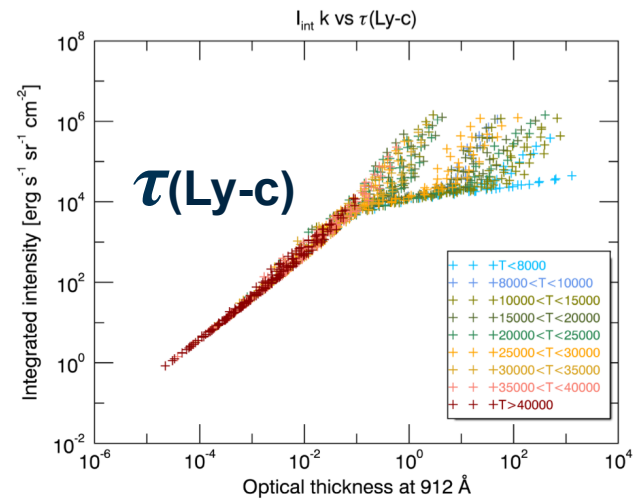
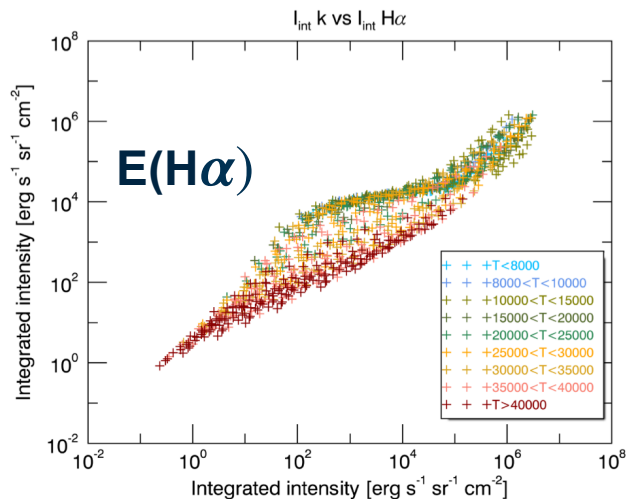
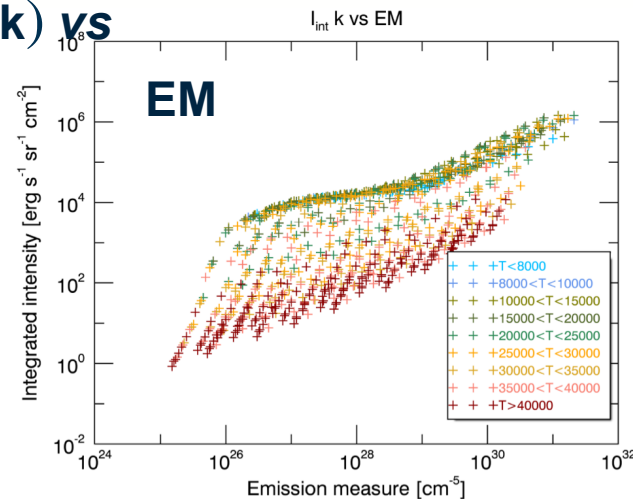
Can be used to estimate size of transition region (Jejcic et al 2019).

Correlations between integrated intensities and central intensities show that LOS variations of plasma parameters are reflected only in integrated intensities

Nicolas Labrosse – Recent results in solar proarr

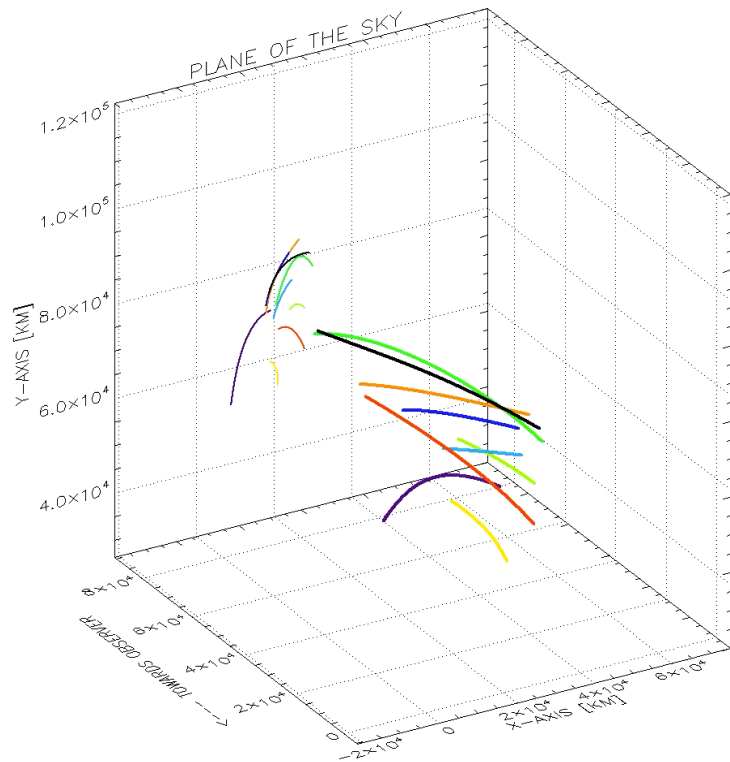
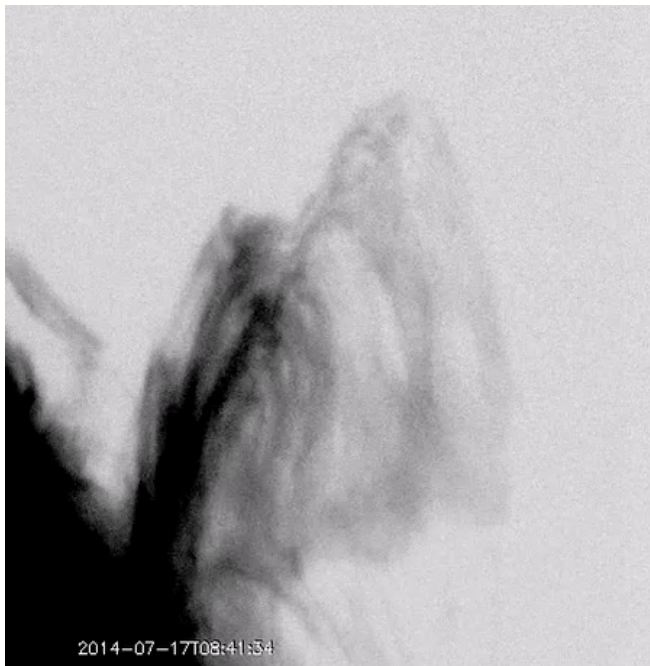


E(Mg II k) vs





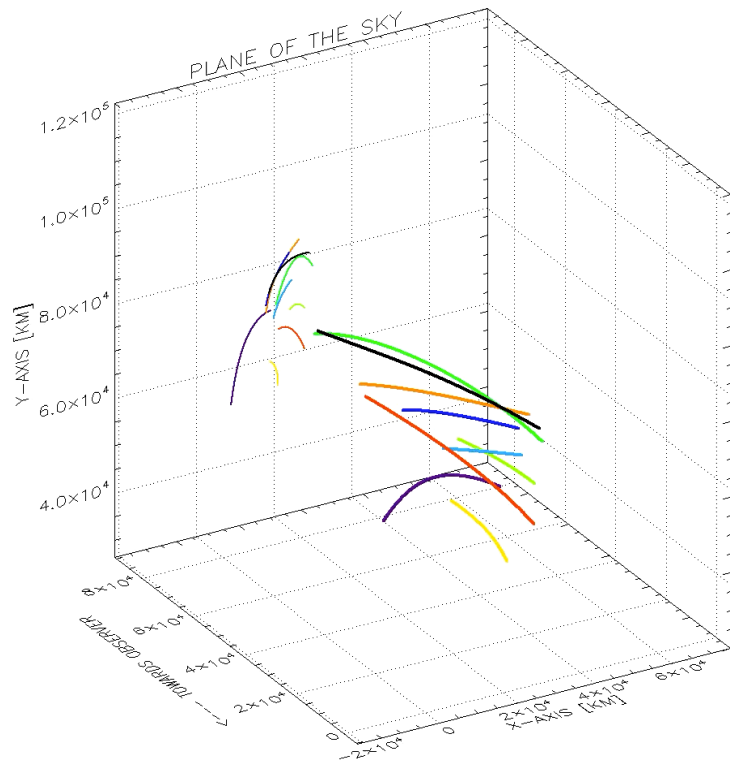
What else did we learn?



Schmieder et al (2017): “The spiral-like structure of the prominence observed in the plane of the sky is mainly due to the projection effect of long arches of threads (up to 8×10^4 km). Knots run along more or less horizontal threads with velocities reaching 65 km s^{-1} .”



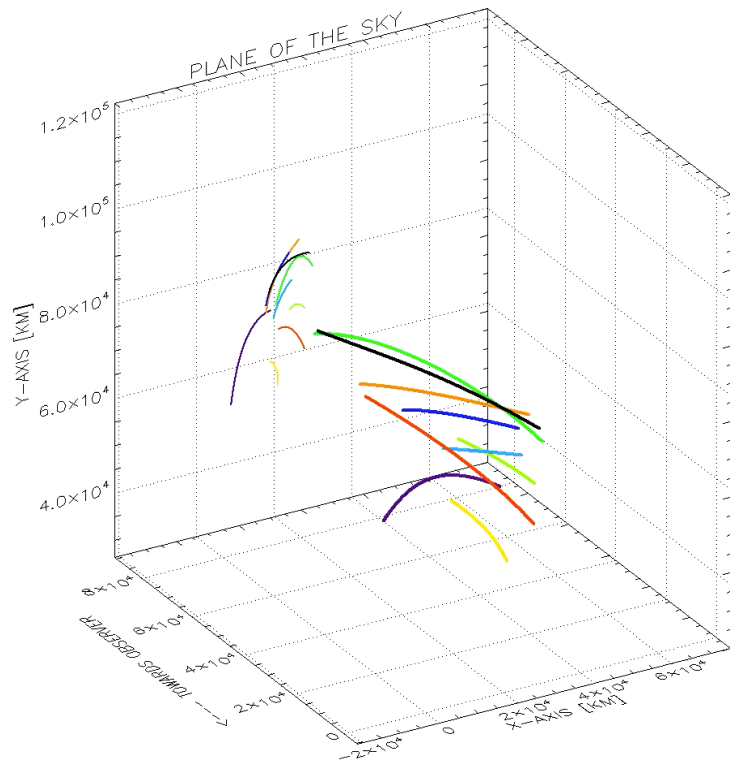
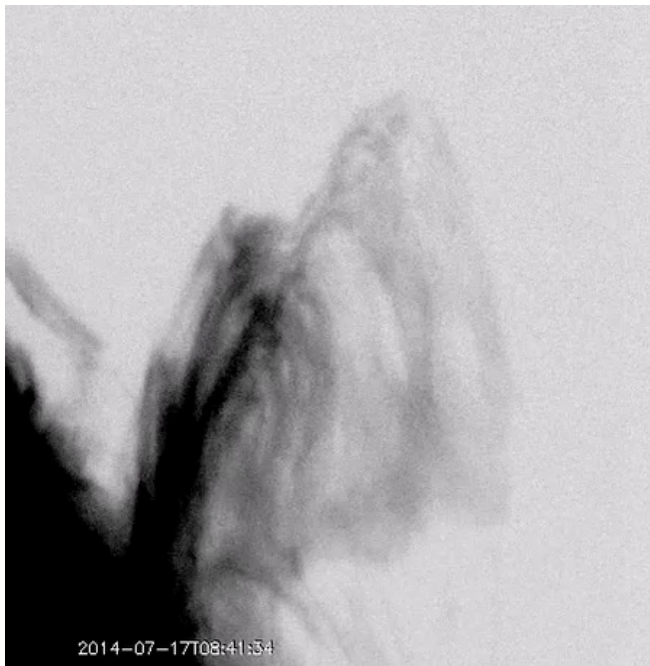
What else did we learn?



Schmieder et al (2017): “The spiral-like structure of the prominence observed in the plane of the sky is mainly due to the projection effect of long arches of threads (up to 8×10^4 km). Knots run along more or less horizontal threads with velocities reaching 65 km s^{-1} .”



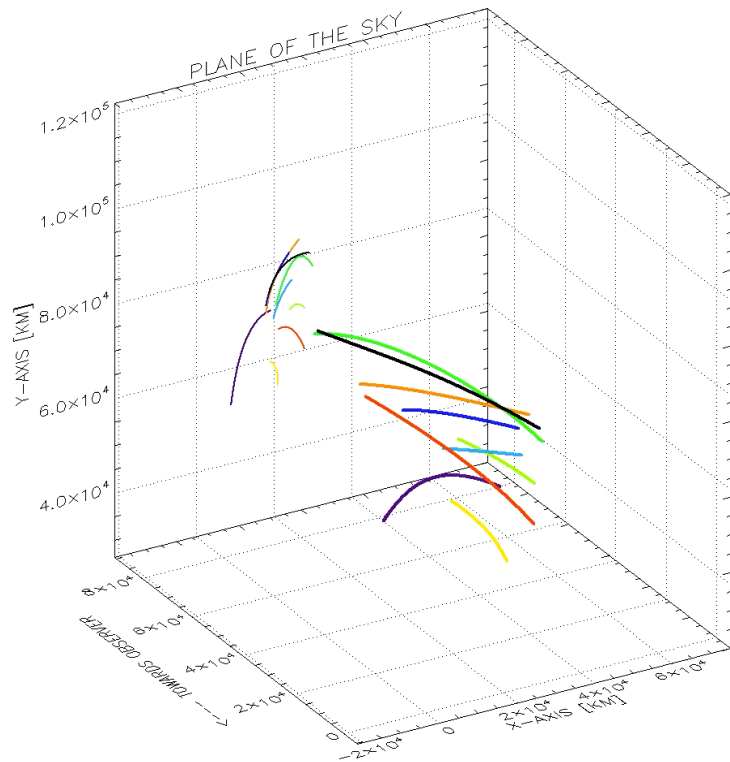
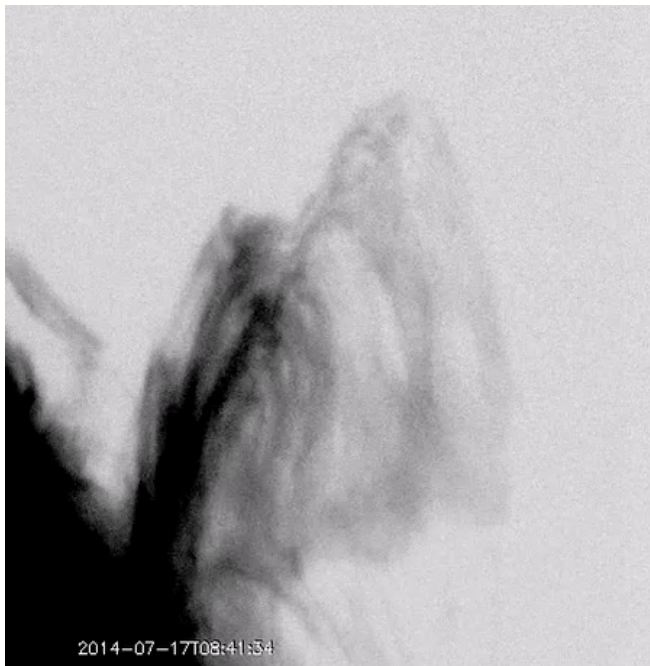
What else did we learn?



Schmieder et al (2017): “The spiral-like structure of the prominence observed in the plane of the sky is mainly due to the projection effect of long arches of threads (up to 8×10^4 km). Knots run along more or less horizontal threads with velocities reaching 65 km s^{-1} .”



What else did we learn?



Schmieder et al (2017): “The spiral-like structure of the prominence observed in the plane of the sky is mainly due to the projection effect of long arches of threads (up to 8×10^4 km). Knots run along more or less horizontal threads with velocities reaching 65 km s^{-1} .”

Prominence dynamics

Schmieder et al (2014)

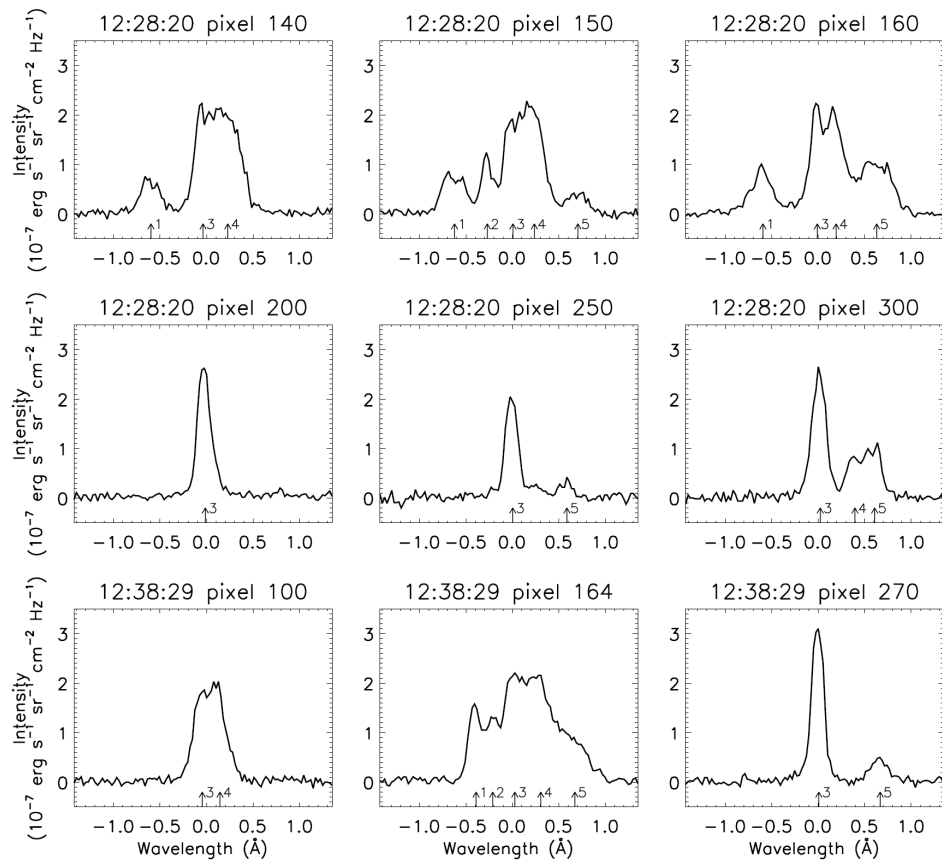
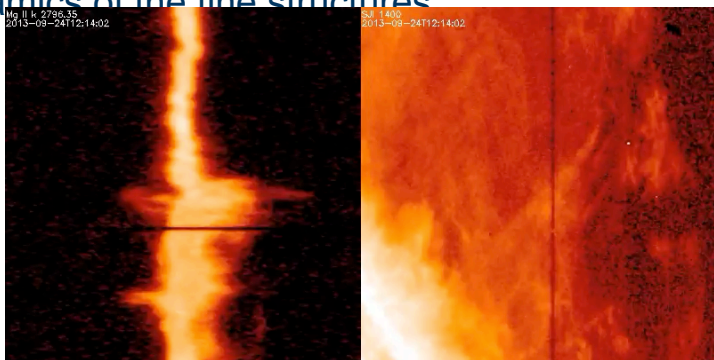
Line profiles along the slit show multiple structures along the line of sight

A relatively static component is always found

In some pixels Doppler shifts of up to 80 km/s are detected

Some pixels have structures with opposite Doppler shifts, suggesting the possibility of counter-streaming flows

IRIS has an excellent spatial, spectral, and temporal resolution, making it possible to observe the dynamics of the fine structures



Prominence dynamics

Schmieder et al (2014)

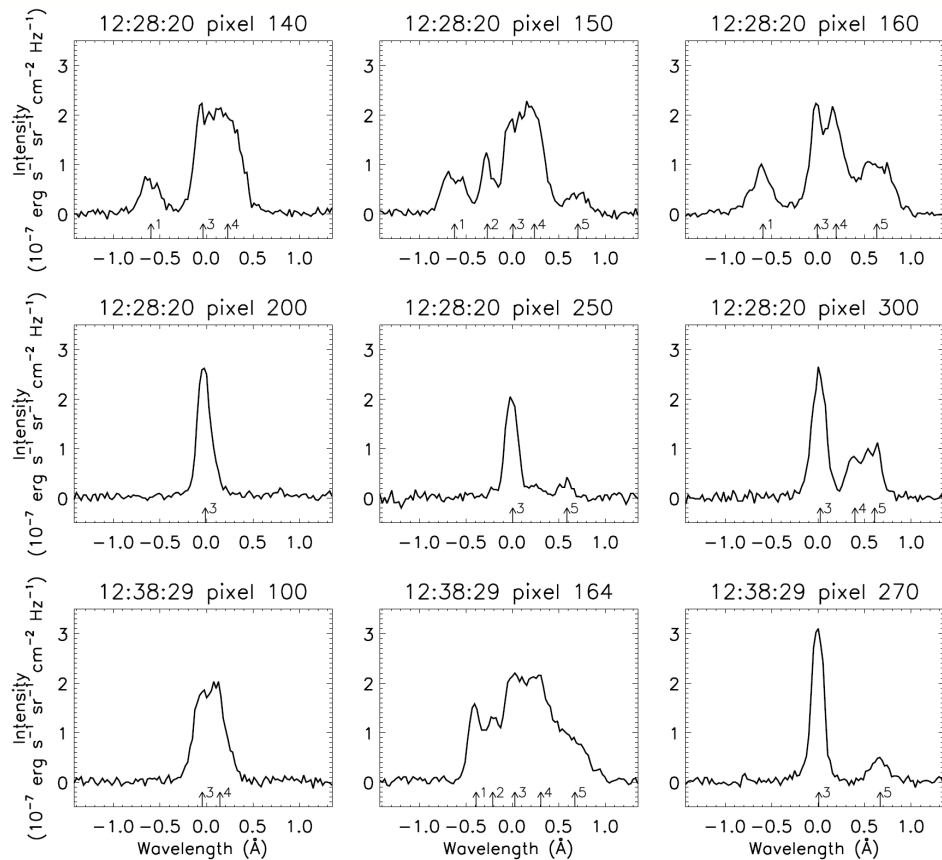
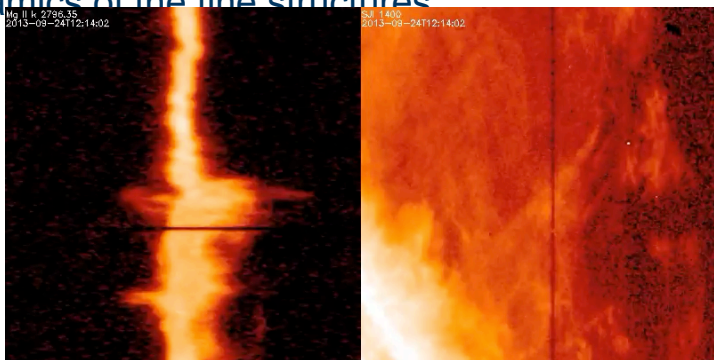
Line profiles along the slit show multiple structures along the line of sight

A relatively static component is always found

In some pixels Doppler shifts of up to 80 km/s are detected

Some pixels have structures with opposite Doppler shifts, suggesting the possibility of counter-streaming flows

IRIS has an excellent spatial, spectral, and temporal resolution, making it possible to observe the dynamics of the fine structures



Prominence dynamics

Schmieder et al (2014)

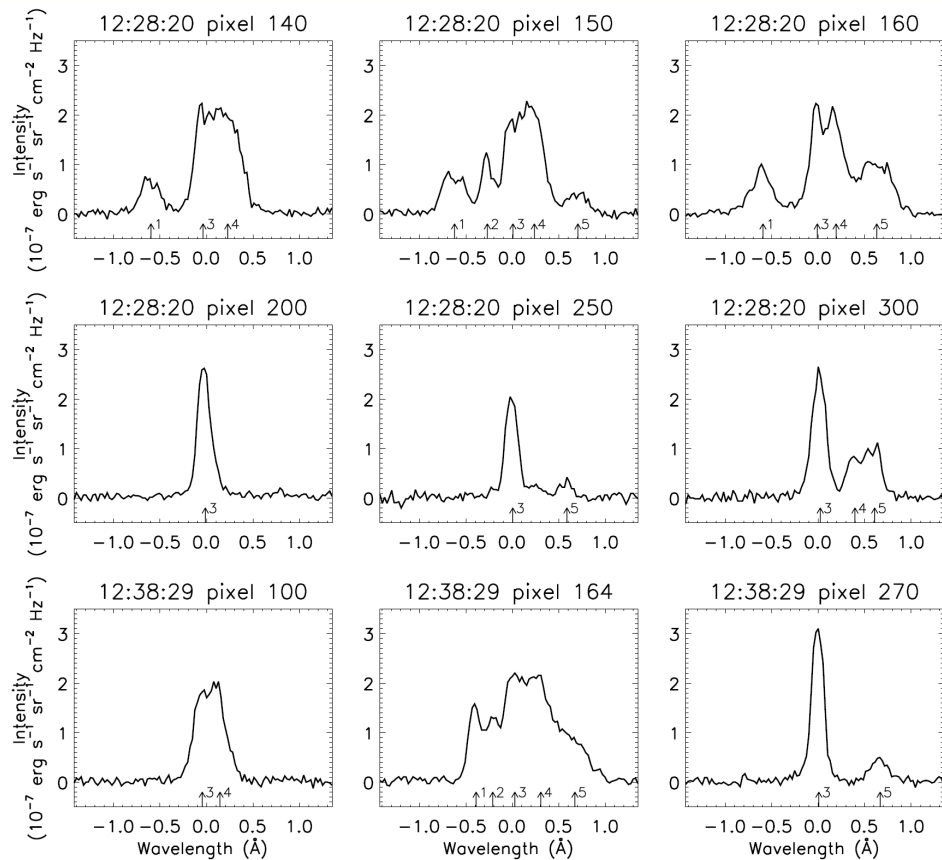
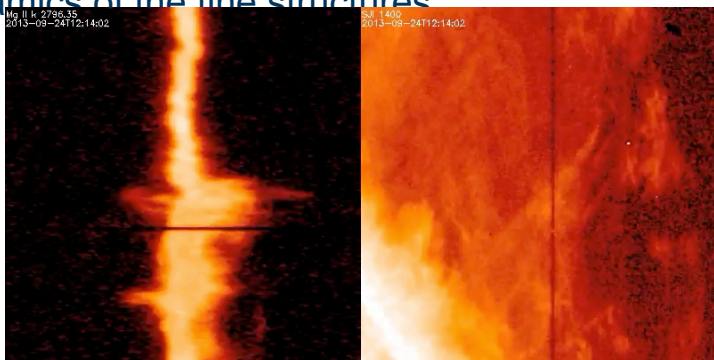
Line profiles along the slit show multiple structures along the line of sight

A relatively static component is always found

In some pixels Doppler shifts of up to 80 km/s are detected

Some pixels have structures with opposite Doppler shifts, suggesting the possibility of counter-streaming flows

IRIS has an excellent spatial, spectral, and temporal resolution, making it possible to observe the dynamics of the fine structures

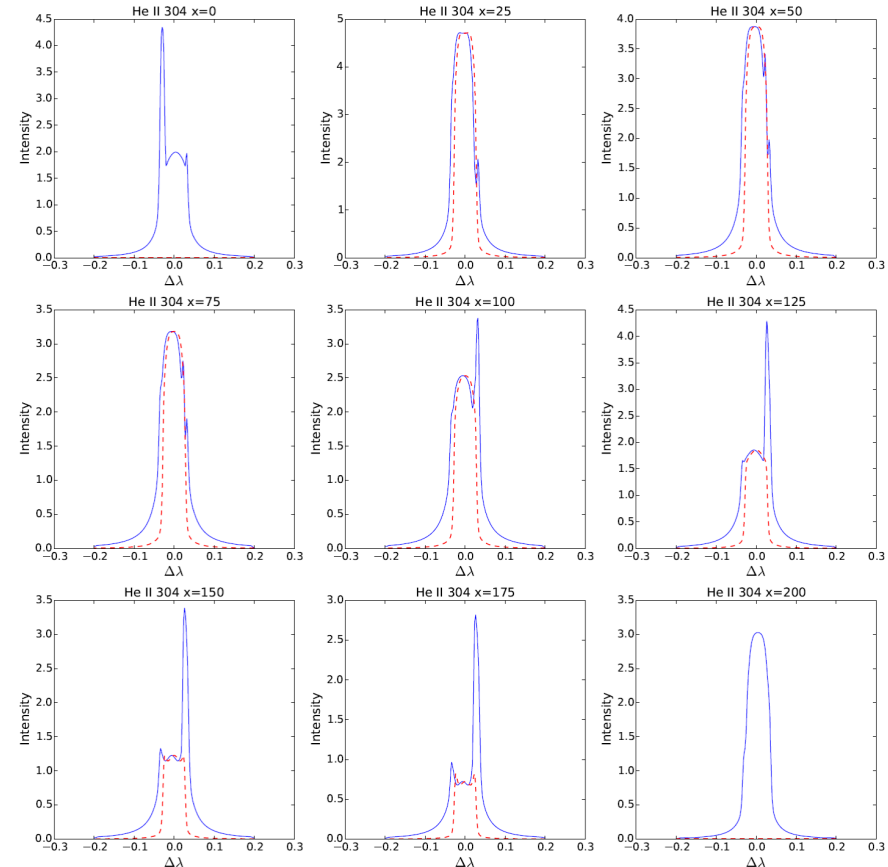


Prominence fine structures

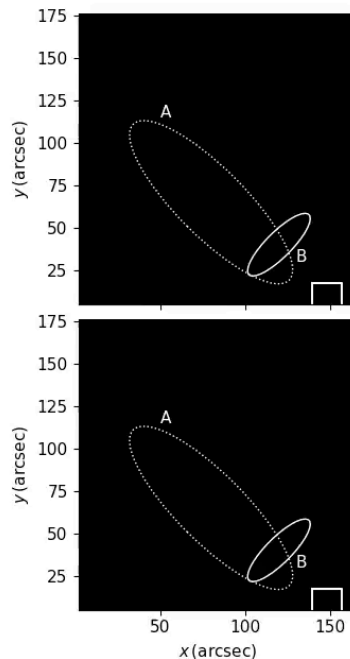
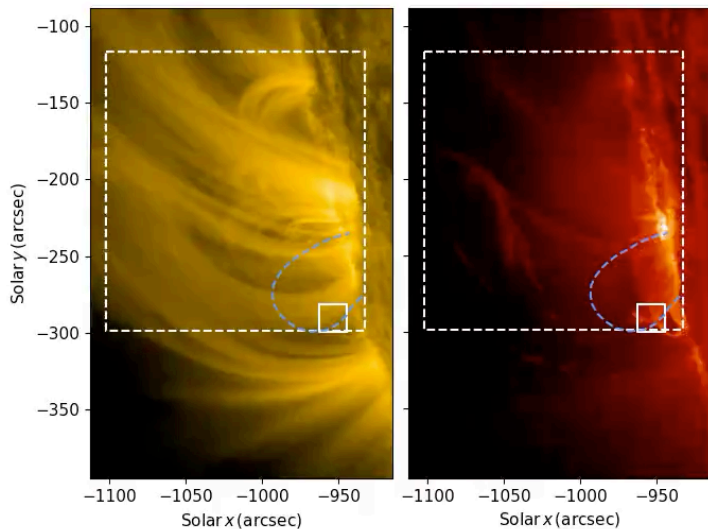
Labrosse & Rodger (2016)

Optically thick line profiles become more complex when the radiation is integrated over several prominence threads moving along the line of sight (Gunar et al 2007, 2008; Labrosse & Rodger 2016).

Multi-thread prominence models are required to reproduce observed Mg II spectra (Schmieder et al 2014, Ruan et al 2018).



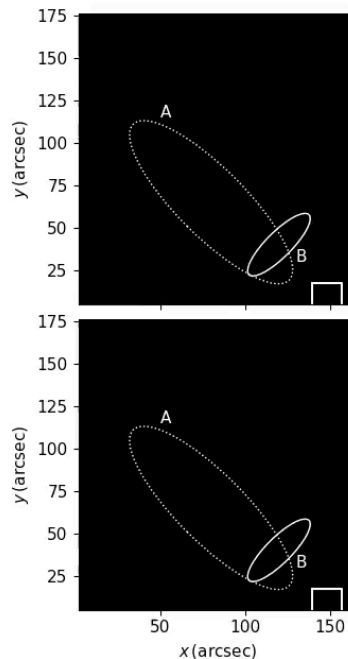
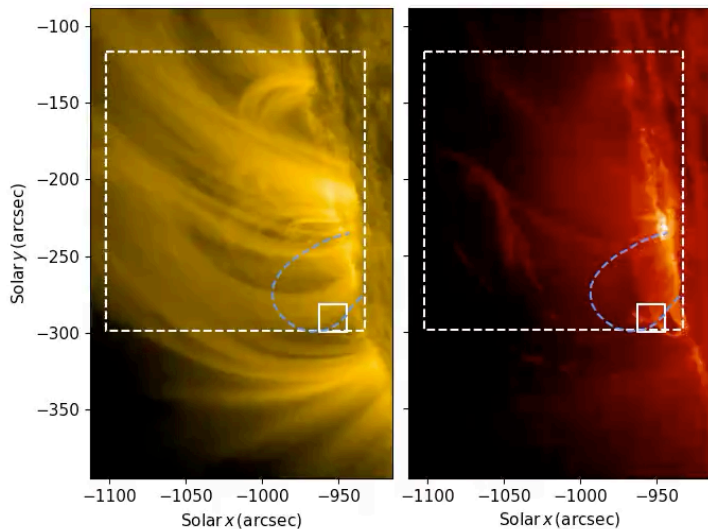
Coronal rain triggered by magnetic reconnection



Can reconnection between threads of a low-lying prominence flux rope and surrounding coronal field lines trigger thermal instability and subsequent formation of condensations?

Kohutova et al (2019)

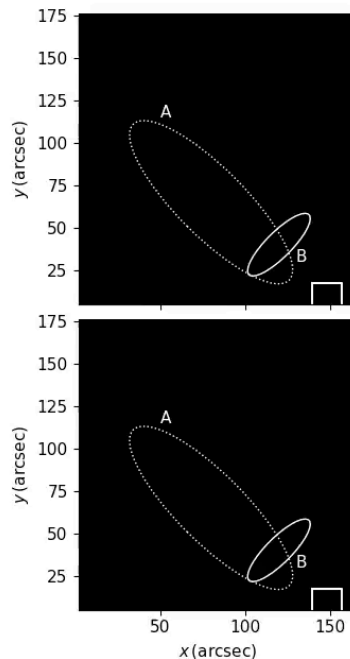
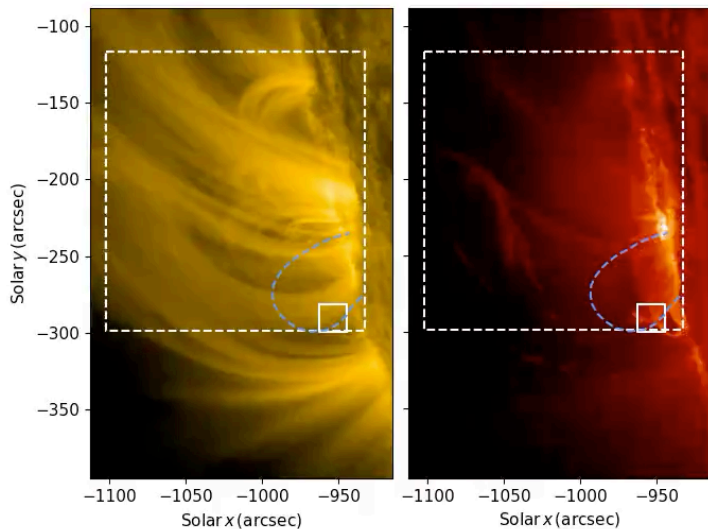
Coronal rain triggered by magnetic reconnection



Can reconnection between threads of a low-lying prominence flux rope and surrounding coronal field lines trigger thermal instability and subsequent formation of condensations?

Kohutova et al (2019)

Coronal rain triggered by magnetic reconnection



Can reconnection between threads of a low-lying prominence flux rope and surrounding coronal field lines trigger thermal instability and subsequent formation of condensations?

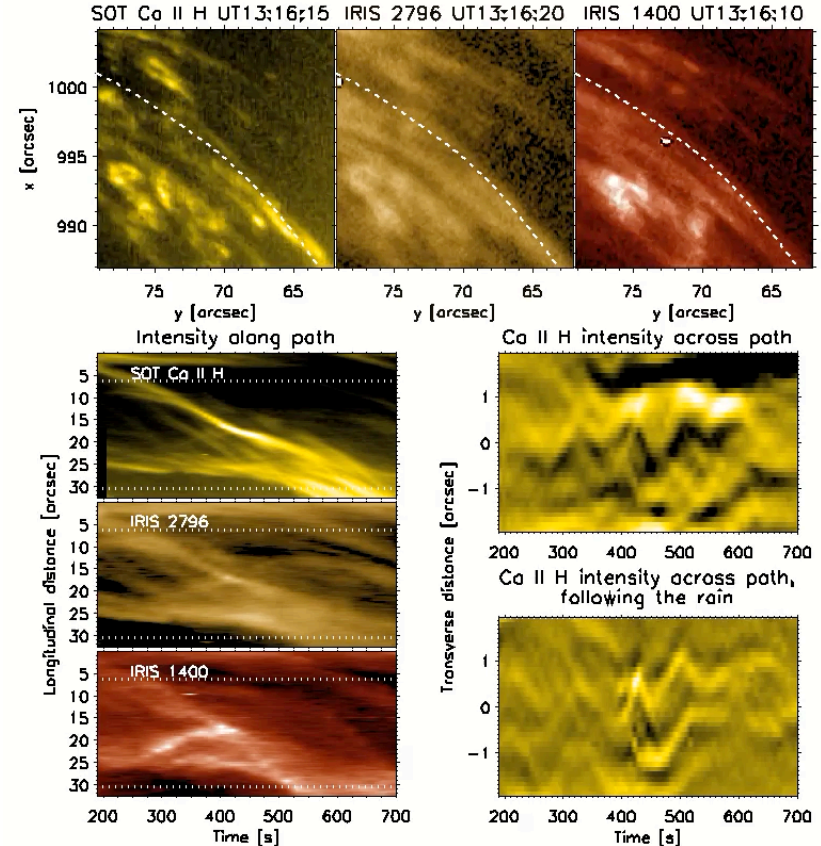
Kohutova et al (2019)

MHD waves generated by colliding flows

Transverse MHD waves may be generated in situ in the corona through flow collision.

More observations are required, over longer time ranges and larger fields-of-view, to assess to what extent these flows and the transverse MHD waves generated in this way contribute to the overall energy balance.

Antolin et al (2018)

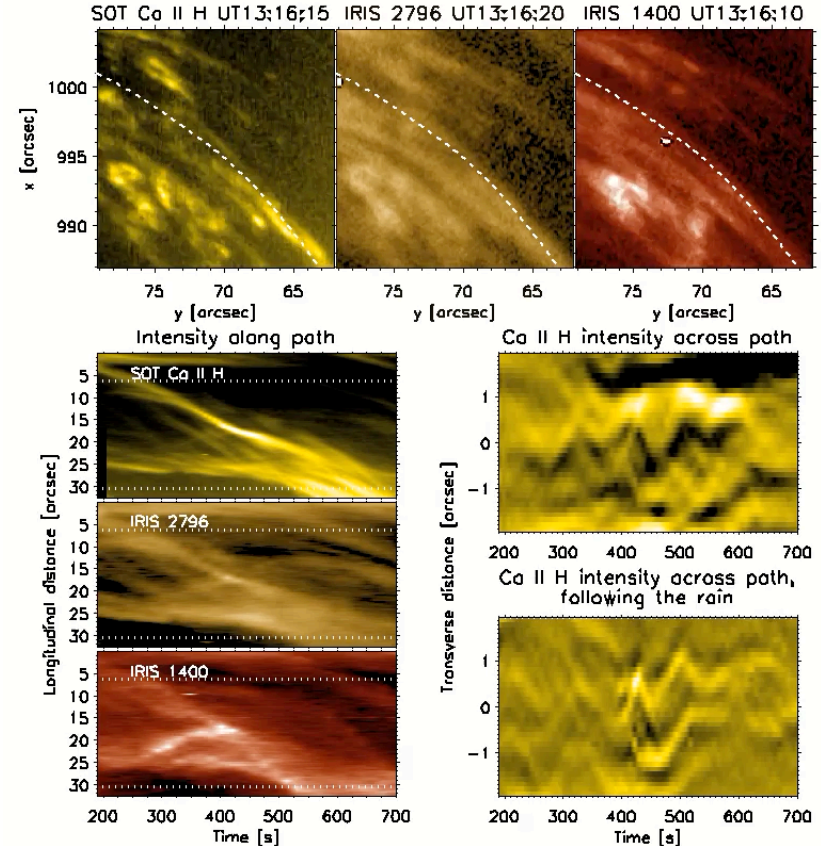


MHD waves generated by colliding flows

Transverse MHD waves may be generated in situ in the corona through flow collision.

More observations are required, over longer time ranges and larger fields-of-view, to assess to what extent these flows and the transverse MHD waves generated in this way contribute to the overall energy balance.

Antolin et al (2018)

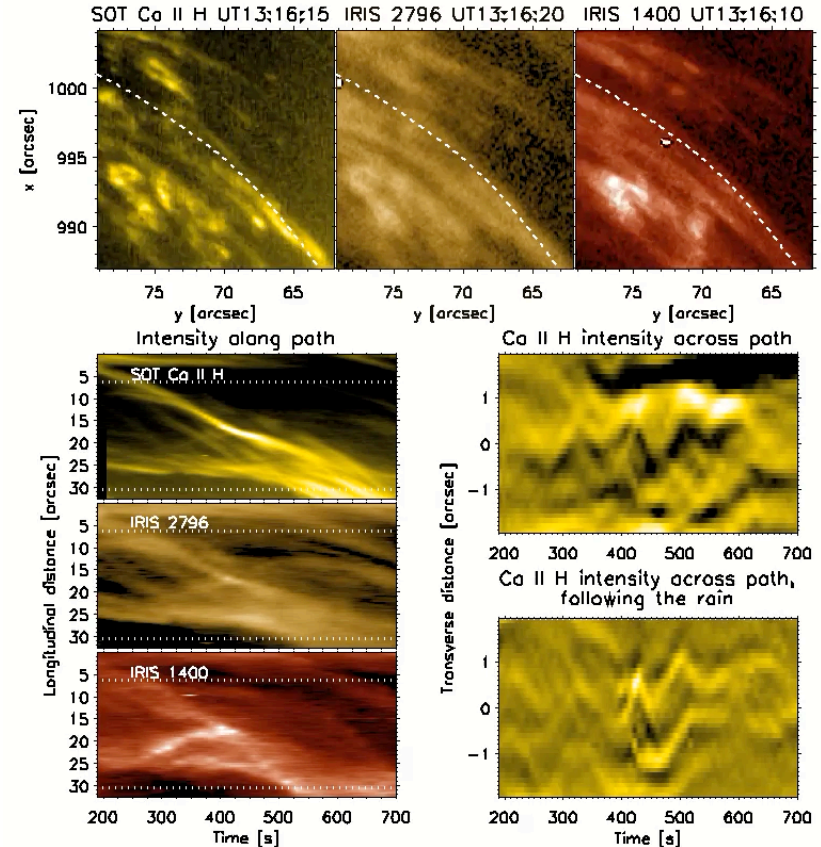


MHD waves generated by colliding flows

Transverse MHD waves may be generated in situ in the corona through flow collision.

More observations are required, over longer time ranges and larger fields-of-view, to assess to what extent these flows and the transverse MHD waves generated in this way contribute to the overall energy balance.

Antolin et al (2018)



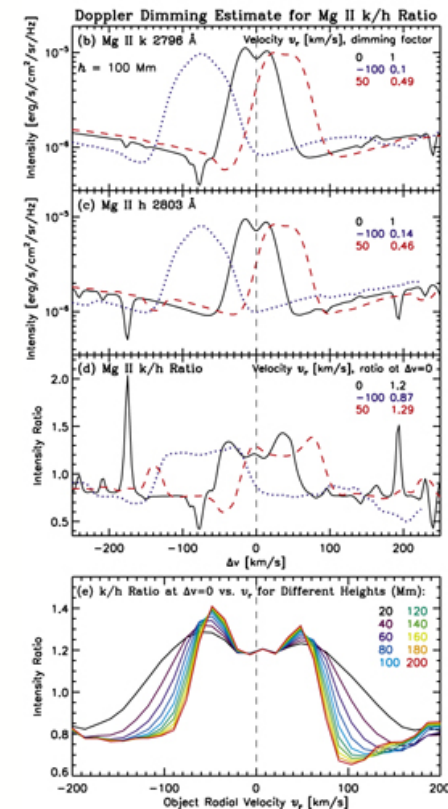
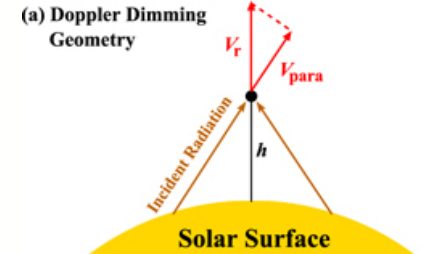
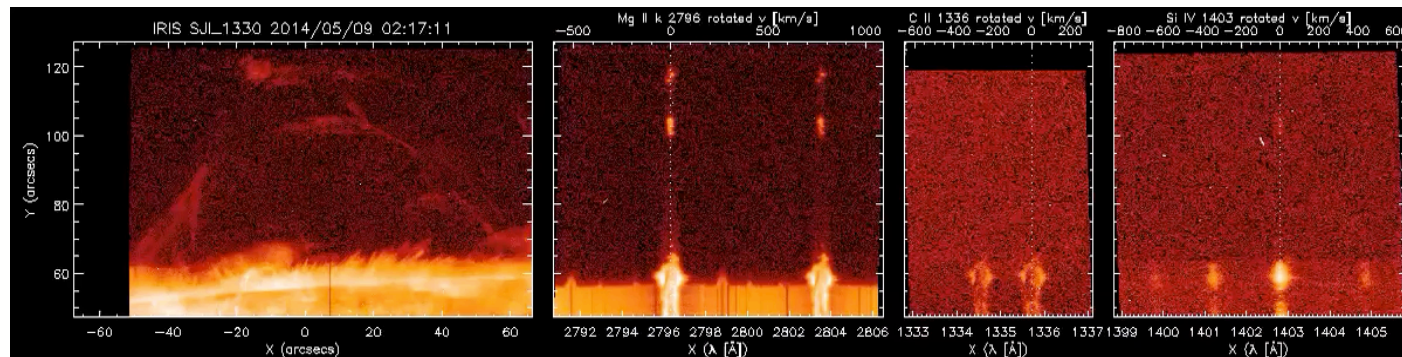


Eruptions

Very low (~ 1.12) k/h intensity ratio in fallback material

Could be explained by Doppler dimming effect \rightarrow Needs to be investigated

Liu et al (2015)



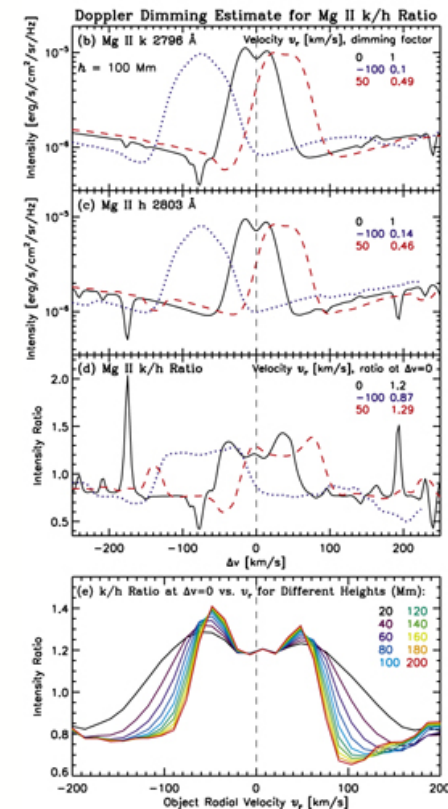
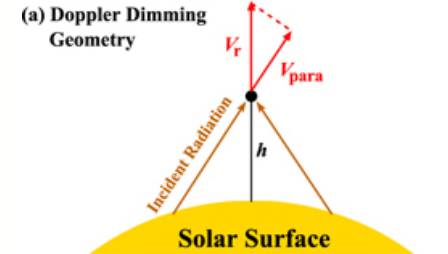
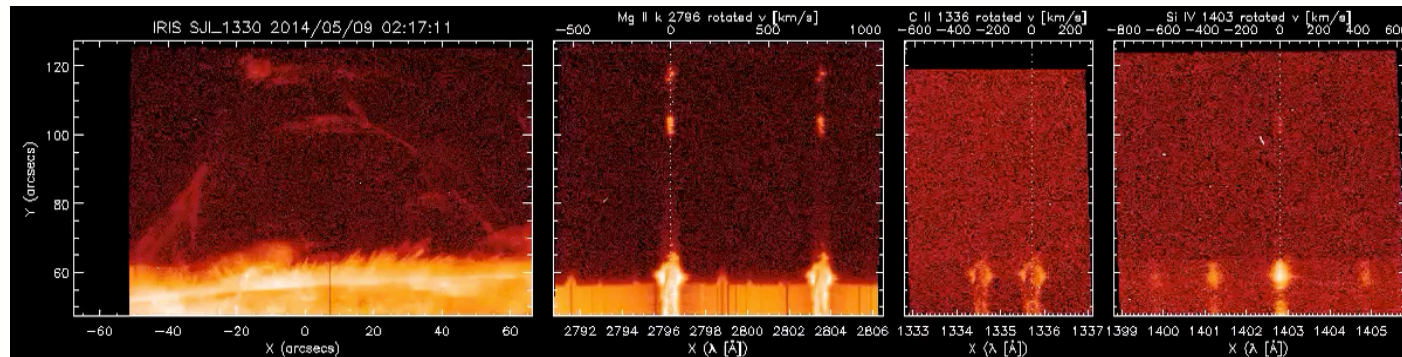


Eruptions

Very low (~ 1.12) k/h intensity ratio in fallback material

Could be explained by Doppler dimming effect \rightarrow Needs to be investigated

Liu et al (2015)



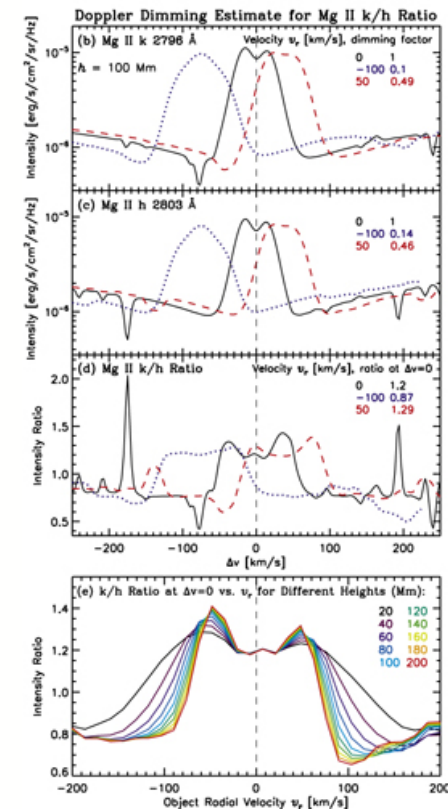
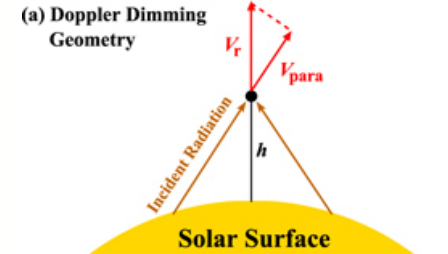
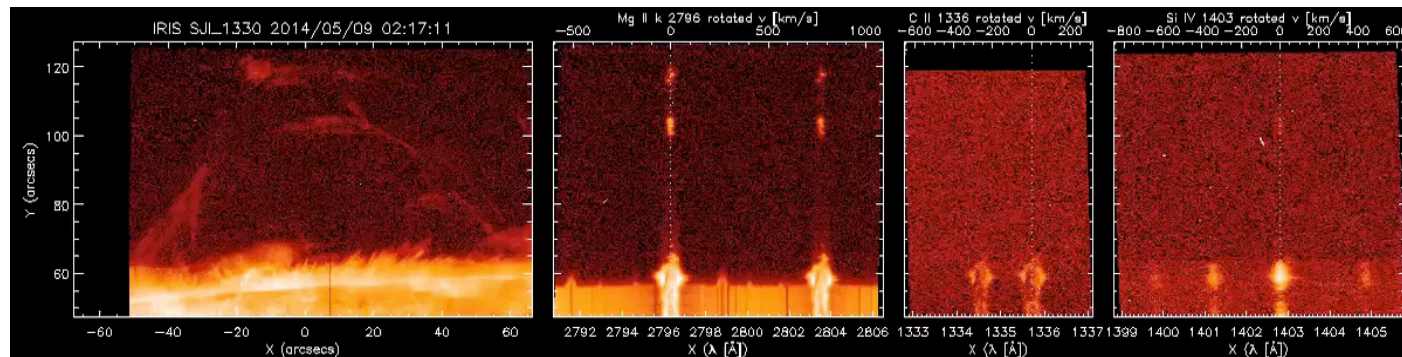


Eruptions

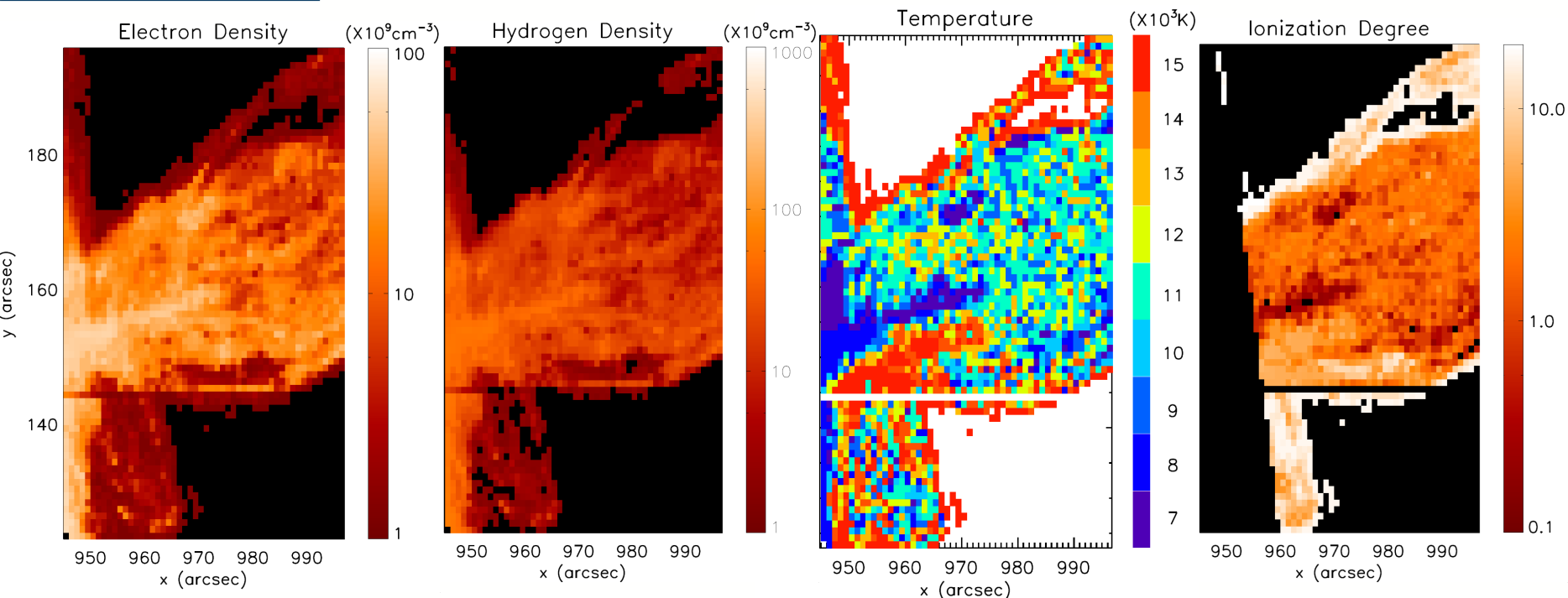
Very low (~ 1.12) k/h intensity ratio in fallback material

Could be explained by Doppler dimming effect \rightarrow Needs to be investigated

Liu et al (2015)



Eruptions and NLTE modelling



Zhang et al (2019) made an attempt to recover plasma parameters in an EP based on comparisons between computed and observed Mg II k & h integrated intensities

Summary

Multi-wavelength observations illustrate how different prominences appear in lines formed at different temperatures, and of different optical thicknesses.

IRIS observations allow us to probe small scales and dynamics of prominences

- Tornadoes, coronal rain, oscillations, are key elements of the prominence evolution

Mg II line features diagnostics:

- k/h ratio \sim temperature
- Line reversals \sim 1/3 of line profiles

Non-LTE modelling essential to interpret Mg II h & k spectra

- Need to consider more sophisticated models, most likely inclusion of a number of 2D moving threads along line-of-sight

High-resolution observations require advanced models

Perspectives

Main objective

to determine the temperature, density, and ionisation degree of the prominence plasma as a whole (integrated along the line of sight) and at the level of its fine-structure threads.

How to achieve this: Advanced 2D NLTE radiative transfer code

- Study the variations of observable spectral features from our models, focusing on small-scale prominence threads of ~ 100 km in size.
- Enable quick interpretation of spectra by provision of electronic tables and plots relating line profiles and intensities (with details on line reversals and peak-to-peak distances for optically thick lines) to key model parameters.
- Establish the ionisation degree structure inside prominence threads resulting from the NLTE solutions to the statistical equilibrium and radiative transfer equations
- Compute spectral line profiles for major ions
- Analysis of and comparisons with observations across multiple wavelengths

Conclusions

IRIS observations bring new insights on prominence structure, and link between plasma properties and observed radiation.

Improvements in high-resolution observations, and availability of new spectral windows, requires continuous development of existing codes

Probing different plasma regions with the usual suspects:

- H α ; Lyman lines; He I D3, 10830, 584 + He II 304; Ca II; Mg II
- “PCTR” lines (CDS, SUMER, IRIS, SPICE)
- FIR, mm thermal continuum (ALMA, DKIST)